Blind channel shortening for asynchronous SC-IFDMA systems with CFOs

Donatella Darsena, *Member, IEEE,* Giacinto Gelli, Luigi Paura, *Member, IEEE,* Francesco Verde, *Member, IEEE,*

***Abstract*—This paper proposes a blind channel shortening algorithm for uplink reception of a single-carrier interleaved frequency-division multiple-access (SC-IFDMA) system transmitting over a highly-dispersive channel, which is affected by both timing offsets (TOs) and frequency offsets (CFOs). When the length of the cyclic prefix (CP) is insufficient to compensate for channel dispersion and TOs, a common strategy is to shorten the channel by means of time-domain equalization, in order to restore CP properties and ease signal reception. The proposed receiver exhibits a three-stage structure: the first stage performs blind shortening of all the user channel impulse responses (CIRs), by adopting the minimum mean-output energy criterion, without requiring neither *a priori* knowledge of the CIRs to be shortened, nor preliminary compensation of the CFOs; the second stage performs joint compensation of the CFOs; finally, to alleviate noise amplification effects, possibly arising from CFO compensation, the third stage implements per-user signal-to-noise ratio (SNR) maximization, without requiring knowledge of the shortened CIRs. A theoretical analysis is carried out to assess the effectiveness of the proposed shortening algorithm in the high-SNR regime; moreover, the performances of the overall receiver are validated and compared with those of existing methods by extensive Monte Carlo computer simulations.**

***Index Terms*—Carrier frequency offset (CFO), channel shortening, minimum-mean-output-energy (MMOE) criterion, multiple access interference (MAI), single-carrier interleaved frequency-division multiple-access (SC-IFDMA), timing offset (TO).**

I. Introduction

AMONG multiple-access schemes for next-generation broadband wireless systems, orthogonal frequency-division multiple-access (OFDMA) [1]–[3] is receiving a significant attention, due to its many appealing features, such as high spectral efficiency and low complexity of transceiver equipments. One of the major drawbacks of OFDMA is due to the large fluctuations of the transmitted signal envelope [4], which dictates the use of expensive linear amplifiers in the uplink, as well as significant power back-off at the user transmitters, thus resulting in both undesirable additional costs and waste of battery power. To overcome this drawback, the *single-carrier interleaved frequency-division multiple-access* (SC-IFDMA) [5] scheme has been recently proposed, which can be interpreted as a precoded version of OFDMA, where the user data blocks are first subject to the Discrete Fourier Transform (DFT), and then assigned to a set of subcarriers that are uniformly chosen over the total available band, so-called interleaved carrier assignment scheme (CAS). SC-IFDMA exhibits lower values of the uplink peak-to-average power ratio, while preserving most of the benefits of OFDMA.

Similarly to OFDMA [6], the performance of the SC-IFDMA uplink is sensitive to time offsets (TOs) and carrier frequency offsets (CFOs) between the user transmitters and the receiver. The combined effects of TOs and CFOs result in both interblock interference (IBI) and loss of orthogonality among subcarriers, which, in turn, generate intercarrier interference (ICI) and multiple access interference (MAI) at the receiver. To overcome this problem, synchronization/compensation techniques originally devised for the OFDMA uplink (see [6] for a survey) can be modified and applied to the SC-IFDMA uplink; moreover, a CFO estimation/compensation scheme targeted for SC-IFDMA systems has been proposed in [7].

Since joint estimation of synchronization parameters for all the users in the OFDMA/SC-IFDMA uplink is a challenging task, it is commonly assumed that each user tries to adapt its transmission, either by exploiting feedback from the base station (BS) or relying on synchronization information acquired in downlink, such that the signals arrive at the BS with only (possibly small) residual TOs and CFOs. For this reason, many papers (e.g., [7]–[10]) assume a timing quasi-synchronous (QS) scenario, wherein the cyclic prefix (CP) can still compensate for the combined effects of the multipath channel dispersion and the residual TO for each user; under this assumption, fine timing synchronization at the BS is avoided and, thus, the task of the receiver reduces to estimating and compensating for the residual CFOs. However, fulfillment of the QS assumption might be impractical for systems operating over highly-dispersive multipath channels: in this case, joint timing and frequency synchronization at the BS is needed, which becomes a formidable task in the case of interleaved CAS, since the users cannot be separated in advance by simple bandpass filtering, as in subband CAS [6].

In this paper, we consider the uplink of SC-IFDMA systems affected by both TOs and CFOs, operating over a highly-dispersive channel for which the QS assumption is violated,

Manuscript received October 3, 2012; revised January 29, 2013 and May 23, 2013; accepted May 31, 2013. The editor coordinating the review of this manuscript and approving it for publication was Prof. Teng Joon Lim.

This work was supported in part by Italian National Projects "DRIVE IN^2" and "HABITAT".

D. Darsena is with the Department for Technologies, Parthenope University, Napoli I-80143, Italy (e-mail: darsena@uniparthenope.it).

G. Gelli, L. Paura, and F. Verde are with the Department of Electrical Engineering and Information Technology, University Federico II, Naples I-80125, Italy [e-mail: (gelli, paura, f.verde)@unina.it].

G. Gelli, L. Paura, and F. Verde are also with Consorzio Nazionale Interuniversitario per le Telecomunicazioni (CNIT), Research Unit of Napoli.

i.e., the CP is not long enough to compensate for channel dispersion plus the residual user TOs.

To the best of our knowledge, such a challenging scenario has not been tackled yet in the technical literature. Our design employs a time-domain equalizer (TEQ) at the BS, working as a *channel shortener*, whose task is to partially equalize the *extended* (i.e., including also the TOs) channels in order to restore the QS condition. Several non-blind [11]–[17] as well as blind [18]–[24] channel-shortening algorithms have been proposed for single-input single-output OFDM systems, some of which have also been extended [25]–[30] to the multiple-input multiple-output case. Non-blind techniques require *a priori* knowledge of the channel impulse responses (CIRs) to be shortened, which can be estimated via the transmission of long training sequences. Blind approaches are more appealing, since no explicit channel estimation procedure is involved. It is worth noting that all the aforementioned techniques were developed for single-user OFDM systems and, except for [20], perfect frequency synchronization is assumed. Recently, a blind multiuser channel shortening method has been proposed [31] for the uplink of an OFDMA system, which can be applied also to SC-IFDMA with minor modifications. The synthesis of the channel shortener in [31] is carried out at the BS separately for each user, on the basis of a frequency-domain cost function and, hence, a fine frequency synchronization step is preliminarily required. The proposed multiuser channel shortener relies instead on the constrained minimum-mean-output-energy (MMOE) [24], [30] criterion and performs joint channel shortening of the user channels in the time-domain, through a single linear transformation of the received data. Compared to the method of [31], our approach is *fully blind*, since neither knowledge of the CIRs to be shortened, nor preliminary estimation of the TOs and CFOs, are required.

The paper is organized as follows. Section II introduces the model for the SC-IFDMA uplink in the presence of both TOs and CFOs. In Section III, the proposed receiver is described, its channel-shortening capabilities in the high-SNR regime are analyzed, and its computational complexity is briefly discussed. Monte Carlo computer simulation results, aimed at assessing the shortening capabilities and the bit-error-rate (BER) performance of the proposed receiver, are presented in Section IV, whereas concluding remarks are drawn in Section V.

A. Notations

The fields of complex, real, and integer numbers are denoted with $\mathbb{C}$, $\mathbb{R}$, and $\mathbb{Z}$, respectively; matrices [vectors] are denoted with upper [lower] case boldface letters (e.g., $\mathbf{A}$ or $\mathbf{a}$); the field of $m\times n$ complex [real] matrices is denoted as $\mathbb{C}^{m\times n}$ [$\mathbb{R}^{m\times n}$], with $\mathbb{C}^m$ [$\mathbb{R}^m$] used as a shorthand for $\mathbb{C}^{m\times 1}$ [$\mathbb{R}^{m\times 1}$]; $\{\mathbf{A}\}_{i,j}$ indicates the $(i+1,j+1)$th element of matrix $\mathbf{A}\in\mathbb{C}^{m\times n}$, with $i\in\{0,1,\ldots,m-1\}$ and $j\in\{0,1,\ldots,n-1\}$; the superscripts $*$, T, H, -1, and $\dagger$ denote the conjugate, the transpose, the conjugate transpose, the inverse, and the Moore-Penrose generalized inverse of a matrix, respectively; the symbol $\star$ stands for (linear) convolution and $\otimes$ denotes Kronecker product of matrices; $\delta(n)$ is the discrete-time unit impulse, i.e., $\delta(n)=1$ for $n=0$ and zero otherwise, $\Pi_P(n)$ is the discrete-time rectangular window, i.e., $\Pi_P(n)=1$ for $n\in\{0,1,\ldots,P-1\}$ and zero otherwise; $\mathbf{0}_m\in\mathbb{R}^m$, $\mathbf{1}_m\in\mathbb{R}^m$, $\mathbf{O}_{m\times n}\in\mathbb{R}^{m\times n}$, and $\mathbf{I}_m\in\mathbb{R}^{m\times m}$ denote the null vector, the vector whose entries are all equal to one, the null matrix, and the identity matrix, respectively; for any $\mathbf{a}\in\mathbb{C}^n$, $\|\mathbf{a}\|$ denotes the Euclidean norm; $\mathrm{rank}(\mathbf{A})$, $\mathcal{N}(\mathbf{A})$, $\mathcal{R}(\mathbf{A})$, and $\mathcal{R}^{\perp}(\mathbf{A})$ denote the rank, the null space, the range (column space), and the orthogonal complement of the column space of $\mathbf{A}\in\mathbb{C}^{m\times n}$ in $\mathbb{C}^m[\mathbb{R}^m]$; given $\mathbf{A}_0,\mathbf{A}_1,\ldots\mathbf{A}_{n-1}\in\mathbb{C}^{m\times m}$, the matrix $\mathbf{A}=\mathrm{diag}(\mathbf{A}_0,\mathbf{A}_1,\ldots\mathbf{A}_{n-1})\in\mathbb{C}^{nm\times nm}$ is block diagonal with ith main diagonal block $\mathbf{A}_i$, for $i\in\{0,1,\ldots,n-1\}$; $\mathrm{rep}_N[f(n)]\triangleq\sum_{k=-\infty}^{+\infty}f(n-kN)$ denotes the replication of period N of $f(n)$; $\lfloor x\rfloor$ is the largest integer not greater than x; $j\triangleq\sqrt{-1}$ is the imaginary unit and the operator $\mathbb{E}[\cdot]$ denotes ensemble averaging.

II. The uplink SC-IFDMA system model

Let us consider the uplink of a SC-IFDMA system with $K\le K_{\mathrm{m}}$ active users, each employing a single-antenna transceiver, transmitting to a common BS equipped with N_{r} antennas. The system employs a total of M subcarriers, divided in K_{m} disjoint sets, each consisting of $M_{\mathrm{u}}\triangleq M/K_{\mathrm{m}}$ subcarriers. In SC-IFDMA, the subcarriers are uniformly assigned (interleaved CAS) over the whole signal band, i.e., let $i_{k,0}<i_{k,1}<\cdots<i_{k,M_{\mathrm{u}}-1}$ denote the subcarriers assigned to user $k\in\{1,2,\ldots K\}$, one has

$$i_{k,\ell}=\ell\,K_{\mathrm{m}}+\phi_k\,,\qquad\text{for }\ell\in\{0,1,\ldots,M_{\mathrm{u}}-1\}\tag{1}$$

where $\phi_k\in\{0,1,\ldots,K_{\mathrm{m}}-1\}$ denotes the index of the first subcarrier allocated to the kth user.

Let $\mathbf{s}_k(n)\triangleq[s_{k,0}(n),s_{k,1}(n),\ldots,s_{k,M_{\mathrm{u}}-1}(n)]^T\in\mathbb{C}^{M_{\mathrm{u}}}$ denote the nth ($n\in\mathbb{Z}$) data block of the kth user: hereinafter, we assume that $\mathbf{s}_k(n)$ is a zero-mean vector having covariance matrix $\mathbb{E}[\mathbf{s}_k(n)\,\mathbf{s}_k^H(n)]=\sigma_s^2\,\mathbf{I}_{M_{\mathrm{u}}}$, with $\mathbf{s}_{k_1}(n_1)$ statistically independent of $\mathbf{s}_{k_2}(n_2)$ for $k_1\neq k_2$ and $n_1\neq n_2$. The vector $\mathbf{s}_k(n)$ is first converted into the frequency domain through DFT, thus obtaining $\widetilde{\mathbf{s}}_k(n)\triangleq\mathbf{W}_{\mathrm{dft}}\,\mathbf{s}_k(n)\in\mathbb{C}^{M_{\mathrm{u}}}$, where $\mathbf{W}_{\mathrm{dft}}\in\mathbb{C}^{M_{\mathrm{u}}\times M_{\mathrm{u}}}$ denotes the M_{u}-point normalized DFT matrix, whose elements are $\{\mathbf{W}_{\mathrm{dft}}\}_{\ell_1,\ell_2}=M_{\mathrm{u}}^{-1/2}e^{-j\frac{2\pi}{M_{\mathrm{u}}}\ell_1\ell_2}$, for $\ell_1,\ell_2\in\{0,1,\ldots,M_{\mathrm{u}}-1\}$. The resulting block $\widetilde{\mathbf{s}}_k(n)$ is then subject to SC-IFDMA subcarrier mapping, followed by M-point IDFT and insertion of a CP of length L_{cp}. Let $P\triangleq M+L_{\mathrm{cp}}$, the obtained time-domain block can be expressed as

$$\begin{aligned}\mathbf{u}_k(n)&\triangleq[u_{k,0}(n),u_{k,1}(n),\ldots,u_{k,P-1}(n)]^T\\&=\mathbf{T}_{\mathrm{cp}}\,\mathbf{W}_k\,\widetilde{\mathbf{s}}_k(n)\in\mathbb{C}^P\end{aligned}\tag{2}$$

where $\mathbf{T}_{\mathrm{cp}}\triangleq[\mathbf{I}_{\mathrm{cp}}^T,\mathbf{I}_M]^T\in\mathbb{R}^{P\times M}$ takes into account CP insertion, with $\mathbf{I}_{\mathrm{cp}}\in\mathbb{R}^{L_{\mathrm{cp}}\times M}$ collecting the last L_{cp} rows of $\mathbf{I}_M$, whereas $\mathbf{W}_k\in\mathbb{C}^{M\times M_{\mathrm{u}}}$ denotes a submatrix of the M-point normalized IDFT matrix, whose elements are $\{\mathbf{W}_k\}_{\ell_1,\ell_2}=M^{-1/2}e^{j\frac{2\pi}{M}\ell_1 i_{k,\ell_2}}$, for $\ell_1\in\{0,1,\ldots,M-1\}$ and $\ell_2\in\{0,1,\ldots,M_{\mathrm{u}}-1\}$. Vector $\mathbf{u}_k(n)$ undergoes parallel-to-serial conversion, and the resulting sequence $u_k(\ell)$ ($\ell\in\mathbb{Z}$), defined by $u_k(nP+p)=u_{k,p}(n)$ for $p\in\{0,1,\ldots,P-1\}$,

feeds a digital-to-analog (D/A) converter operating at rate $1/T_c = P/T$, where T denotes the symbol length.

Under the assumption that in-phase/quadrature-phase (I/Q) imbalance [32] in the frequency upconversion (at the transmitters) and frequency downconversion (at the receiver) is negligibly small,[1] the baseband received signal at the αth BS antenna ($\alpha \in \{1, 2, \ldots, N_\mathrm{r}\}$) can be written as

$$r_\alpha(t) = \sum_{k=1}^{K} e^{j2\pi\Delta f_k t} \left[u_k(t - \Delta\tau_k) \star h_{k,\alpha}(t)\right] + w_\alpha(t) \quad (3)$$

where $u_k(t) = \sum_{\ell=-\infty}^{+\infty} u_k(\ell)\, \delta(t - \ell\, T_c)$ is the baseband signal of the kth user before the transmitting filter, $h_{k,\alpha}(t)$ is the *composite* CIR (encompassing the cascade of the transmitting filter, multipath channel, and receiving filter) between the kth user transmitter and the αth BS antenna receiver, Δf_k and $\Delta\tau_k$ denote the residual CFO and TO of the kth user, respectively, and $w_\alpha(t)$ takes into account thermal noise.

We assume hereinafter that $h_{k,\alpha}(t)$ spans L_k sampling periods, i.e., $h_{k,\alpha}(t) \equiv 0$ for $t \notin [0, L_k\, T_c]$. Moreover, by assuming that each user tries to adjust its uplink synchronization parameters, the residual TO is either much smaller than L_k or, in the worst case, reduces to the two-way propagation delay [6] between the kth user and the BS, whereas the residual CFO is limited to one-half of the subcarrier spacing $\Delta f_0 = 1/(MT_c)$, i.e., $|\Delta f_k| < \Delta f_0/2$. It is convenient to express each TO as $\Delta\tau_k = \theta_k\, T_c + \xi_k$, where $\theta_k > 0$ and $\xi_k \in [0, T_c)$ are the integer and fractional components of $\Delta\tau_k$ with respect to T_c, respectively, and define the *normalized* CFO $\epsilon_k \triangleq \Delta f_k/\Delta f_0$, such that $|\epsilon_k| < 1/2$.

At each antenna, the signal (3) is sampled at rate N_c/T_c, with $N_\mathrm{c} \geq 1$ denoting the oversampling factor. Accounting for (3), the qth sample of the signal received at the αth antenna in the time interval $[mT_c, mT_c + T_c)$ is given by

$$\begin{aligned} r_\alpha^{(q)}(m) &\triangleq r_\alpha\left(m\, T_c + q\frac{T_c}{N_\mathrm{c}}\right) \\ &= \sum_{k=1}^{K} e^{j\frac{2\pi}{M}\epsilon_k m} \sum_{\ell=0}^{L_k+\theta_k} h_{k,\alpha}^{(q)}(\ell - \theta_k)\, u_k(m - \ell) + w_\alpha^{(q)}(m) \end{aligned} \quad (4)$$

with $m \in \mathbb{Z}$ and $q \in \{0, 1, \ldots, N_\mathrm{c} - 1\}$, where

$$\begin{aligned} h_{k,\alpha}^{(q)}(\ell) &\triangleq e^{j\frac{2\pi}{M N_\mathrm{c}}\epsilon_k q}\, h_{k,\alpha}(\ell\, T_c + q\, T_c/N_\mathrm{c} - \xi_k) \\ w_\alpha^{(q)}(m) &\triangleq w_\alpha(m\, T_c + q\, T_c/N_\mathrm{c})\,. \end{aligned}$$

Let $Q \triangleq N_\mathrm{r}\, N_\mathrm{c}$, a compact single-input multiple-output model can be obtained by collecting the N_c data vectors resulting from oversampling over all the N_r receiving antennas into the Q-dimensional complex vector

$$\mathbf{r}(m) \triangleq [\{\mathbf{r}^{(0)}(m)\}^T, \{\mathbf{r}^{(1)}(m)\}^T, \ldots, \{\mathbf{r}^{(N_\mathrm{c}-1)}(m)\}^T]^T$$

with $\mathbf{r}^{(q)}(m) \triangleq [r_1^{(q)}(m), r_2^{(q)}(m), \ldots, r_{N_\mathrm{r}}^{(q)}(m)]^T \in \mathbb{C}^{N_\mathrm{r}}$, for $q \in \{0, 1, \ldots, N_\mathrm{c} - 1\}$, thus obtaining

$$\mathbf{r}(m) = \sum_{k=1}^{K} e^{j\frac{2\pi}{M}\epsilon_k m} \sum_{\ell=0}^{L_k+\theta_k} \mathbf{h}_k(\ell)\, u_k(m - \ell) + \mathbf{w}(m) \quad (5)$$

where

$$\begin{aligned} \mathbf{h}_k(\ell) &\triangleq [\{\mathbf{h}_k^{(0)}(\ell)\}^T, \{\mathbf{h}_k^{(1)}(\ell)\}^T, \ldots, \{\mathbf{h}_k^{(N_\mathrm{c}-1)}(\ell)\}^T]^T \\ \mathbf{w}(m) &\triangleq [\{\mathbf{w}^{(0)}(m)\}^T, \{\mathbf{w}^{(1)}(m)\}^T, \ldots, \{\mathbf{w}^{(N_\mathrm{c}-1)}(m)\}^T]^T \end{aligned}$$

are Q-dimensional complex vectors, with

$$\begin{aligned} \mathbf{h}_k^{(q)}(\ell) &\triangleq [h_{k,1}^{(q)}(\ell - \theta_k), h_{k,2}^{(q)}(\ell - \theta_k), \ldots, h_{k,N_\mathrm{r}}^{(q)}(\ell - \theta_k)]^T \\ \mathbf{w}^{(q)}(m) &\triangleq [w_1^{(q)}(m), w_2^{(q)}(m), \ldots, w_{N_\mathrm{r}}^{(q)}(m)]^T \end{aligned}$$

for $q \in \{0, 1, \ldots, N_\mathrm{c} - 1\}$, are N_r-dimensional complex vectors. In the sequel, we assume that $\mathbf{w}(m)$ is a zero-mean vector having covariance matrix $\mathbb{E}[\mathbf{w}(m)\, \mathbf{w}^H(m)] = \sigma_w^2\, \mathbf{I}_Q$, which is statistically independent of $u_k(m)$, for each $k \in \{1, 2, \ldots K\}$, and with $\mathbf{w}(m_1)$ uncorrelated with $\mathbf{w}(m_2)$ for $m_1 \neq m_2$. It is noteworthy that (5) describes a perfectly time-synchronized SC-IFDMA uplink, wherein the order of the kth channel is extended from L_k to $L_k + \theta_k$.

III. The Proposed Blind Multiuser Channel Shortening Receiver

Let $L_\mathrm{max} \triangleq \max_{k\in\{1,2,\ldots,K\}} \{L_k + \theta_k\}$, when $L_\mathrm{max} > L_\mathrm{cp}$ the effects of channel dispersion and TOs cannot be completely eliminated by CP removal, which, coupled with the presence of CFOs, introduces a severe performance degradation, due to the simultaneous presence of IBI, ICI, and MAI. To overcome this drawback, we propose to incorporate in the receiver a multiuser TEQ, aimed at shortening the overall CIRs (encompassing also the TOs), thus enabling effective IBI suppression through CP removal. Such a choice will simplify the subsequent CFO estimation/compensation algorithm, which operates on IBI-free data and suppresses ICI and MAI by restoring subcarrier orthogonality.

A. Blind multiuser MMOE channel shortening

The proposed L_e-order finite-impulse response (FIR) TEQ operates on $L_\mathrm{e} + 1$ consecutive samples of $\mathbf{r}(m)$ given by (5), gathered in vector

$$\overline{\mathbf{r}}(m) \triangleq [\mathbf{r}^T(m), \mathbf{r}^T(m-1), \ldots, \mathbf{r}^T(m - L_\mathrm{e})]^T \in \mathbb{C}^{Q\,(L_\mathrm{e}+1)}$$

which can be expressed, taking into account (5), as

$$\overline{\mathbf{r}}(m) = \sum_{k=1}^{K} e^{j\frac{2\pi}{M}\epsilon_k m}\, \mathbf{\Sigma}_k\, \mathbf{H}_k\, \overline{\mathbf{u}}_k(m) + \overline{\mathbf{w}}(m) \quad (6)$$

where

$$\begin{aligned} \mathbf{\Sigma}_k &\triangleq \mathbf{I}_Q \otimes \mathrm{diag}(1, e^{-j\frac{2\pi}{M}\epsilon_k}, \ldots, e^{-j\frac{2\pi}{M}\epsilon_k L_\mathrm{e}}) \\ \overline{\mathbf{u}}_k(m) &\triangleq [u_k(m), u_k(m-1), \ldots, u_k(m - L_\mathrm{g})]^T \\ \overline{\mathbf{w}}(m) &\triangleq [\mathbf{w}^T(m), \mathbf{w}^T(m-1), \ldots, \mathbf{w}^T(m - L_\mathrm{e})]^T \end{aligned}$$

and the block Toeplitz channel matrix $\mathbf{H}_k \in \mathbb{C}^{Q(L_\mathrm{e}+1)\times(L_\mathrm{g}+1)}$ is shown at the top of the next page, with $L_\mathrm{g} \triangleq L_\mathrm{e} + L_\mathrm{max}$.

[1] Negligible I/Q distortion can be obtained [33] by employing traditional superheterodyne architectures to convert the baseband signal to a radio frequency signal and vice versa.

$$\mathbf{H}_k \triangleq \begin{bmatrix} \mathbf{h}_k(0) & \mathbf{h}_k(1) & \dots & \mathbf{h}_k(L_{\max}) & \mathbf{0}_Q & \dots & \mathbf{0}_Q \\ \mathbf{0}_Q & \mathbf{h}_k(0) & \mathbf{h}_k(1) & \dots & \mathbf{h}_k(L_{\max}) & \ddots & \mathbf{0}_Q \\ \vdots & \ddots & \ddots & \ddots & \ddots & \ddots & \mathbf{0}_Q \\ \mathbf{0}_Q & \dots & \ddots & \mathbf{h}_k(0) & \mathbf{h}_k(1) & \dots & \mathbf{h}_k(L_{\max}) \end{bmatrix} \tag{7}$$

Since the synthesis of the MMOE TEQ depends on second-order statistics of $\overline{\mathbf{r}}(m)$, it is interesting to investigate the properties of its covariance matrix

$$\mathbf{R}_{\overline{\mathbf{r}}\overline{\mathbf{r}}}(m) \triangleq \mathbb{E}[\overline{\mathbf{r}}(m)\,\overline{\mathbf{r}}^H(m)] \in \mathbb{C}^{Q(L_{\rm e}+1)\times Q(L_{\rm e}+1)} \ .$$

It is shown in Appendix A that $\mathbf{R}_{\overline{\mathbf{r}}\overline{\mathbf{r}}}(m)$ is periodically time-varying (PTV) in m with period P, but turns out to be time-invariant [i.e., $\mathbf{R}_{\overline{\mathbf{r}}\overline{\mathbf{r}}}(m) \equiv \mathbf{R}_{\overline{\mathbf{r}}\overline{\mathbf{r}}}$] for the interleaved CAS given by (1), provided that $L_{\rm g} < M_{\rm u}$: such an assumption, which simplifies our design, limits the number of users to a maximum of $K < M/L_g$. The resulting TEQ turns out to be time-invariant,[2] and its output is given by $y(m) = \mathbf{f}^H\,\overline{\mathbf{r}}(m)$, where $\mathbf{f} \in \mathbb{C}^{Q\,(L_{\rm e}+1)}$ is the TEQ weight vector. Accounting for (6) and defining $v(m) \triangleq \mathbf{f}^H\overline{\mathbf{w}}(m)$, one has

$$y(m) = \sum_{k=1}^{K} e^{j\,\frac{2\pi}{M}\epsilon_k m}\,\mathbf{g}_k^H\,\overline{\mathbf{u}}_k(m) + v(m) \tag{8}$$

where $\mathbf{g}_k \triangleq \mathbf{H}_k^H\,\mathbf{\Sigma}_k^H\mathbf{f} \in \mathbb{C}^{L_{\rm g}+1}$ is the *combined* $L_{\rm g}$-order FIR channel-TEQ response of the kth user.

Perfect channel shortening amounts to design the TEQ such that the shortened CIRs of all users are FIR channels of order $L_{\rm eff} \le L_{\rm cp}$ ($L_{\rm eff}$ being a design parameter), i.e., their supports belong to the *desired window* $\{0, 1, \dots, L_{\rm eff}\}$, which assures perfect IBI cancellation after CP removal. To elaborate, let us decompose (8) as the sum of a desired and undesired component: by partitioning

$$\begin{aligned} \overline{\mathbf{u}}_k(m) &= [\overline{\mathbf{u}}_{k,\rm win}(m)^T, \overline{\mathbf{u}}_{k,\rm wall}(m)^T]^T \\ \mathbf{g}_k &= [\mathbf{g}_{k,\rm win}^T, \mathbf{g}_{k,\rm wall}^T]^T \end{aligned} \tag{9}$$

with $\overline{\mathbf{u}}_{k,\rm win}(m) \in \mathbb{C}^{L_{\rm eff}+1}$, $\overline{\mathbf{u}}_{k,\rm wall}(m) \in \mathbb{C}^{L_{\rm g}-L_{\rm eff}}$, $\mathbf{g}_{k,\rm win} \in \mathbb{C}^{L_{\rm eff}+1}$, and $\mathbf{g}_{k,\rm wall} \in \mathbb{C}^{L_{\rm g}-L_{\rm eff}}$ denoting as in [11] the signal/channel components at the TEQ output that are inside and outside the desired window, respectively, the TEQ output (8) can be rewritten as $y(m) = y_{\rm win}(m) + y_{\rm wall}(m)$, with

$$y_{\rm win}(m) = \sum_{k=1}^{K} e^{j\,\frac{2\pi}{M}\epsilon_k m}\,\mathbf{g}_{k,\rm win}^H\,\overline{\mathbf{u}}_{k,\rm win}(m) \tag{10}$$

$$y_{\rm wall}(m) = \sum_{k=1}^{K} e^{j\,\frac{2\pi}{M}\epsilon_k m}\,\mathbf{g}_{k,\rm wall}^H\,\overline{\mathbf{u}}_{k,\rm wall}(m) + v(m)\ . \tag{11}$$

We refer to (11) as the undesired contribution since it contains, besides noise, the IBI component outside the desired window, which cannot be suppressed by CP removal. A simple design criterion would be to constrain $\mathbf{g}_{k,\rm wall} = \mathbf{0}_{L_{\rm g}-L_{\rm eff}}$, which results in the *perfect channel shortening condition*:

$$\mathbf{g}_k = \mathbf{H}_k^H\,\mathbf{\Sigma}_k^H\mathbf{f} = [\mathbf{g}_{k,\rm win}^T, \mathbf{0}_{L_{\rm g}-L_{\rm eff}}^T]^T \qquad \forall k \in \{1, 2, \dots, K\}\,. \tag{12}$$

Eq. (12) can be directly solved for $\mathbf{f}$ (zero-forcing approach), which would require knowledge of $\mathbf{H}_k$ (i.e., of the CIRs to be shortened) and $\mathbf{\Sigma}_k$ (i.e., of the CFOs) and, hence, cannot be implemented blindly. The proposed MMOE approach, instead, forces (12) to be satisfied in a blind manner, by generalizing to the SC-IFDMA scenario the designs of [23], [24], [30], originally proposed for a single-user and perfectly-synchronized ($\Delta\tau_k = \Delta f_k = 0$) OFDM systems. In particular, the vector $\mathbf{f}$ is chosen so as to minimize the mean output-energy MOE($\mathbf{f}$) $\triangleq \mathbb{E}[|y(m)|^2] = \mathbf{f}^H\,\mathbf{R}_{\overline{\mathbf{r}}\overline{\mathbf{r}}}\,\mathbf{f}$ at the TEQ output, with suitable constraints aimed at preserving the desired component (10), which amounts[3] to minimizing $\mathbb{E}[|y_{\rm wall}(m)|^2]$.

To set the blind constraints, let $\mathbf{H}_k = [\mathbf{H}_{k,\rm win}, \mathbf{H}_{k,\rm wall}]$, with

$$\begin{aligned} \mathbf{H}_{k,\rm win} &\triangleq [\mathbf{h}_{k,0}, \mathbf{h}_{k,1}, \dots, \mathbf{h}_{k,L_{\rm eff}}] \in \mathbb{C}^{Q(L_{\rm e}+1)\times(L_{\rm eff}+1)} \\ \mathbf{H}_{k,\rm wall} &\triangleq [\mathbf{h}_{k,L_{\rm eff}+1}, \mathbf{h}_{k,L_{\rm eff}+2}, \dots, \mathbf{h}_{k,L_{\rm g}}] \in \mathbb{C}^{Q(L_{\rm e}+1)\times(L_{\rm g}-L_{\rm eff})} \end{aligned}$$

and observe that $\mathbf{g}_{k,\rm win}$ and $\mathbf{g}_{k,\rm wall}$ in (10), (11) can be expressed as $\mathbf{g}_{k,\rm win}^H = \mathbf{f}^H\,\mathbf{\Sigma}_k\,\mathbf{H}_{k,\rm win}$ and $\mathbf{g}_{k,\rm wall}^H = \mathbf{f}^H\,\mathbf{\Sigma}_k\,\mathbf{H}_{k,\rm wall}$, respectively. Provided that $L_{\rm eff} \in \{0, 1, \dots, \min(L_{\rm e}, L_{\max})\}$, it can be shown [30] that the $(\delta+1)$th column $\mathbf{h}_{k,\delta}$ of $\mathbf{H}_{k,\rm win}$, with $\delta \in \{0, 1, \dots, L_{\rm eff}\}$, can be parameterized as $\mathbf{h}_{k,\delta} = \mathbf{\Theta}_\delta\,\boldsymbol{\xi}_{k,\delta}$, where

$$\mathbf{\Theta}_\delta = [\mathbf{I}_{Q(\delta+1)}, \mathbf{O}_{Q(L_{\rm e}-\delta)\times Q(\delta+1)}^T]^T \in \mathbb{R}^{Q(L_{\rm e}+1)\times Q(\delta+1)}$$

is a *known* full-column rank matrix, which does not depend on k and satisfies $\mathbf{\Theta}_\delta^T\,\mathbf{\Theta}_\delta = \mathbf{I}_{Q(\delta+1)}$, whereas

$$\boldsymbol{\xi}_{k,\delta} = [\mathbf{h}_k^T(\delta), \mathbf{h}_k^T(\delta-1), \dots, \mathbf{h}_k^T(0)]^T \in \mathbb{C}^{Q(\delta+1)}$$

collects samples of the kth CIR to be shortened. Consequently, the $(\delta+1)$th column of $\mathbf{\Sigma}_k\,\mathbf{H}_k$ can be parameterized as $\mathbf{\Sigma}_k\,\mathbf{h}_{k,\delta} = \mathbf{\Sigma}_k\,\mathbf{\Theta}_\delta\,\boldsymbol{\xi}_{k,\delta} = \mathbf{\Theta}_\delta\,\overline{\mathbf{\Sigma}}_{k,\delta}\,\boldsymbol{\xi}_{k,\delta}$, where

$$\overline{\mathbf{\Sigma}}_{k,\delta} \triangleq \mathbf{I}_Q \otimes \mathrm{diag}(1, e^{-j\,\frac{2\pi}{M}\epsilon_k}, \dots, e^{-j\,\frac{2\pi}{M}\epsilon_k\delta})\,.$$

Moreover, since the recursive relation $\mathbf{\Theta}_{\delta-1} = \mathbf{\Theta}_\delta\,\mathbf{J}_\delta$, with $\mathbf{J}_\delta \triangleq [\mathbf{I}_{Q\delta}, \mathbf{O}_{Q\times Q\delta}^T]^T \in \mathbb{C}^{Q(\delta+1)\times Q\delta}$, holds for every value of $\delta \in \{1, 2, \dots, L_{\rm eff}\}$, $\mathbf{g}_{k,\rm win}^H$ can be rewritten as

$$\begin{aligned} \mathbf{g}_{k,\rm win}^H = \mathbf{f}^H\,\mathbf{\Theta}_{L_{\rm eff}}\,[&\mathbf{J}_{L_{\rm eff}}\cdots\mathbf{J}_1\,\overline{\mathbf{\Sigma}}_{k,0}\,\boldsymbol{\xi}_{k,0}, \\ &\mathbf{J}_{L_{\rm eff}}\cdots\mathbf{J}_2\,\overline{\mathbf{\Sigma}}_{k,1}\,\boldsymbol{\xi}_{k,1}, \dots, \overline{\mathbf{\Sigma}}_{k,L_{\rm eff}}\,\boldsymbol{\xi}_{k,L_{\rm eff}}] \end{aligned}$$

[2]When $L_{\rm g} \ge M_{\rm u}$, or for other CASs, such as, e.g., subband CAS [6], the channel shortener turns out to be a PTV filter [35], [36] of period P, whose implementation complexity might be burdensome for large values of P.

[3]To prevent signal cancellation effects [37] in MMOE optimization, it is crucial that $\mathbf{R}_{\overline{\mathbf{u}}_k\overline{\mathbf{u}}_k} \triangleq \mathbb{E}[\overline{\mathbf{u}}(m)\overline{\mathbf{u}}^H(m)]$ be nonsingular: in Appendix A, it is shown that, provided that $L_{\rm g} < M_{\rm u}$, one has $\mathbf{R}_{\overline{\mathbf{u}}_k\overline{\mathbf{u}}_k} = \sigma_s^2\,\mathbf{I}_{L_{\rm e}+1}$ for interleaved CAS, which is trivially nonsingular.

which shows that the desired term (10) can be preserved by imposing the constraint $\mathbf{f}^H \boldsymbol{\Theta}_{L_{\text{eff}}} = \boldsymbol{\gamma}^H$, with $\boldsymbol{\gamma} \in \mathbb{C}^{Q(L_{\text{eff}}+1)}$ a nonzero vector. The blind constrained minimization of MOE($\mathbf{f}$) can thus be written as

$$\mathbf{f}_{\text{mmoe}} = \arg\min_{\mathbf{f}} \left\{ \mathbf{f}^H \mathbf{R}_{\overline{\mathbf{r}}\overline{\mathbf{r}}} \mathbf{f} \right\} \quad \text{subject to} \quad \mathbf{f}^H \boldsymbol{\Theta}_{L_{\text{eff}}} = \boldsymbol{\gamma}^H \tag{13}$$

where, since $\boldsymbol{\Theta}_{L_{\text{eff}}}$ is a known deterministic matrix, the constraint does not require knowledge of the CIRs to be shortened, nor preliminary estimation/compensation of the CFOs. Loosely speaking, left multiplication of the block Toeplitz channel matrix $\mathbf{H}_k$ by the block diagonal matrix $\boldsymbol{\Sigma}_k$, which depends on the CFOs, does not prevent blind parameterization of the columns of $\mathbf{H}_k$, which is hence exploited to preserve the user signals within the desired window while minimizing the mean output-energy. Solution of (13) can be expressed [24] in factored form as $\mathbf{f}_{\text{mmoe}} = \mathbf{F}_{\text{mmoe}} \boldsymbol{\gamma}$, with

$$\mathbf{F}_{\text{mmoe}} = \mathbf{R}_{\overline{\mathbf{r}}\overline{\mathbf{r}}}^{-1} \boldsymbol{\Theta}_{L_{\text{eff}}} \left(\boldsymbol{\Theta}_{L_{\text{eff}}}^T \mathbf{R}_{\overline{\mathbf{r}}\overline{\mathbf{r}}}^{-1} \boldsymbol{\Theta}_{L_{\text{eff}}} \right)^{-1} \in \mathbb{C}^{Q(L_{\text{e}}+1) \times Q(L_{\text{eff}}+1)}. \tag{14}$$

Note that $\mathbf{F}_{\text{mmoe}}$ does not depend on the user index k, and its synthesis needs only knowledge of $\mathbf{R}_{\overline{\mathbf{r}}\overline{\mathbf{r}}}$, which can be consistently estimated from the received data either in batch mode or adaptively [24].

As regards the asymptotic (i.e., when the noise is vanishingly small) channel shortening capabilities of the proposed method, we state the following theorem:

Theorem 1: Let $\boldsymbol{\Pi} \in \mathbb{R}^{Q(L_{\text{e}}+1) \times Q(L_{\text{e}}-L_{\text{eff}})}$ obey $\boldsymbol{\Pi}^T \boldsymbol{\Theta}_{L_{\text{eff}}} = \mathbf{O}_{Q(L_{\text{e}}-L_{\text{eff}}) \times Q(L_{\text{eff}}+1)}$, with $\boldsymbol{\Pi}^T \boldsymbol{\Pi} = \mathbf{I}_{Q(L_{\text{e}}-L_{\text{eff}})}$, and let

$$\mathbf{H}_{\text{wall}} \triangleq [\boldsymbol{\Sigma}_1 \mathbf{H}_{1,\text{wall}}, \ldots, \boldsymbol{\Sigma}_K \mathbf{H}_{K,\text{wall}}] \in \mathbb{C}^{Q(L_{\text{e}}+1) \times K(L_{\text{g}}-L_{\text{eff}})}.$$

For $L_{\text{eff}} \in \{0, 1, \ldots, \min(L_{\text{e}}, L_{\max})\}$, assuming $L_{\text{g}} < M_{\text{u}}$, if the following three conditions hold:

(c1) $Q > K$
(c2) $Q\,(L_{\text{e}} - L_{\text{eff}}) \geq K\,(L_{\text{g}} - L_{\text{eff}})$
(c3) $\text{rank}(\boldsymbol{\Pi}^T \mathbf{H}_{\text{wall}}) = K\,(L_{\text{g}} - L_{\text{eff}})$

then, for $\sigma_s^2/\sigma_w^2 \to +\infty$ and $\forall k \in \{1, 2, \ldots, K\}$, the MMOE combined channel-TEQ impulse response $\mathbf{g}_k = \mathbf{H}_k^H \boldsymbol{\Sigma}_k^H \mathbf{f}_{\text{mmoe}}$ of the kth user satisfies the perfect channel shortening condition (12), with

$$\mathbf{g}_{k,\text{win}} = \mathbf{G}_{k,\text{win}}^{\infty} \boldsymbol{\gamma} \in \mathbb{C}^{L_{\text{eff}}+1}$$
$$\mathbf{G}_{k,\text{win}}^{\infty} \triangleq \mathbf{H}_{k,\text{win}}^H \boldsymbol{\Sigma}_k^H \boldsymbol{\Theta}_{L_{\text{eff}}} \in \mathbb{C}^{(L_{\text{eff}}+1) \times Q(L_{\text{eff}}+1)}$$

for any nonzero $\boldsymbol{\gamma} \in \mathbb{C}^{Q(L_{\text{eff}}+1)}$.

Proof: See Appendix B. ∎

Theorem 1 provides sufficient conditions assuring that the proposed MMOE channel shortener is asymptotically able to jointly shorten the CIRs of *all* the users. Remembering that $Q = N_{\text{r}} N_{\text{c}}$, the assumption $L_{\text{g}} < M_{\text{u}}$ and condition **(c1)** jointly limit the maximum number of users; in particular, **(c1)** shows that, even though oversampling is not strictly necessary when $N_{\text{r}} > K$, values of $N_{\text{c}} > 1$ allow one to accommodate a larger number of users. Moreover, the choice $N_{\text{c}} > 1$ has also a favorable impact on the maximum order of the extended CIR that can be shortened. Indeed, assuming that **(c1)** holds and remembering that $L_{\text{g}} = L_{\text{e}} + L_{\max}$, **(c2)** imposes the following upper bound on $L_{\max}$:

$$L_{\max} \leq (L_{\text{e}} - L_{\text{eff}}) \left(\frac{N_{\text{r}} N_{\text{c}}}{K} - 1 \right) \tag{15}$$

which shows that $L_{\max}$ linearly increases both with the ratio $(N_{\text{r}} N_{\text{c}})/K$ and with $L_{\text{e}} - L_{\text{eff}}$. It is worth remembering that, to achieve IBI suppression, the value of L_{eff} must be chosen such that $L_{\text{eff}} \leq L_{\text{cp}}$. Thus, for a given L_{e}, choosing L_{eff} much smaller than L_{cp} enables shortening of longer channels; this choice, however, might introduce, as discussed in [24], [30], excessive noise enhancement during the channel shortening process; typically, a good trade-off is obtained by choosing $L_{\text{eff}} = L_{\text{cp}}$. Additionally, we note that suitable settings of the TEQ parameters (L_{eff} and L_{e}) require only upper bounds (rather than the exact knowledge) on the channel orders and residual TOs of users. Finally, if **(c1)** and **(c2)** are met, **(c3)** is satisfied with probability one by any matrix $\mathbf{H} \triangleq [\boldsymbol{\Sigma}_1 \mathbf{H}_1, \boldsymbol{\Sigma}_2 \mathbf{H}_2, \ldots, \boldsymbol{\Sigma}_K \mathbf{H}_K]$ having nonzero statistically independent entries drawn from a continuous probability distribution.

Relying on factorization $\mathbf{f}_{\text{mmoe}} = \mathbf{F}_{\text{mmoe}} \boldsymbol{\gamma}$ and defining $\mathbf{z}(m) \triangleq \mathbf{F}_{\text{mmoe}}^H \overline{\mathbf{r}}(m) \in \mathbb{C}^{Q(L_{\text{eff}}+1)}$, the output of the MMOE TEQ can be rewritten as $y_{\text{mmoe}}(m) \triangleq \mathbf{f}_{\text{mmoe}}^H \overline{\mathbf{r}}(m) = \boldsymbol{\gamma}^H \mathbf{z}(m) = \mathbf{z}^T(m) \boldsymbol{\gamma}^*$. Since Theorem 1 ensures that perfect channel shortening is asymptotically achieved for *any* nonzero $\boldsymbol{\gamma}$, the latter expression suggests that multiuser CFO compensation can be directly performed on $\mathbf{z}^T(m)$, before multiplying it by $\boldsymbol{\gamma}^*$. Nevertheless, the choice of $\boldsymbol{\gamma}$ has a significant impact on the system performance: simulation results non reported here show that simple choices (like, e.g., $\boldsymbol{\gamma} = [1, \ldots, 1]^T$) generally lead to poor performances. For this reason, optimization of $\boldsymbol{\gamma}$ will be carried out *after* CFO compensation.

B. Blind multiuser CFO compensation

We consider the CFO estimation/compensation problem, by exploiting algorithms proposed in the literature for interleaved CAS that work *after* CP removal (i.e., on the IBI-free signal). In particular, CFO compensation restores subcarrier orthogonality, allowing thus ICI and MAI to be easily suppressed. Estimation of the CFOs can be obtained e.g. by resorting to existing blind algorithms [7]- [10] or [38], which do not require transmission of reference symbols. Since CFO estimation is outside the scope of the paper, we assume herein that the CFOs have been perfectly estimated, by deferring to numerical simulations in Section IV the analysis of the effects of possible estimation errors. Compensation of the CFOs can be carried out through, e.g., linear multiuser detection algorithms [6]: such a processing can be performed either in the frequency domain [9] or in the time domain [7]. In the following, we pursue the time-domain approach of [7], since it exhibits a lower computational complexity compared to [9].

Although Theorem 1 in Subsection III-A states that perfect channel shortening is achieved only for vanishingly small noise, simulation results of Section IV show that satisfactory

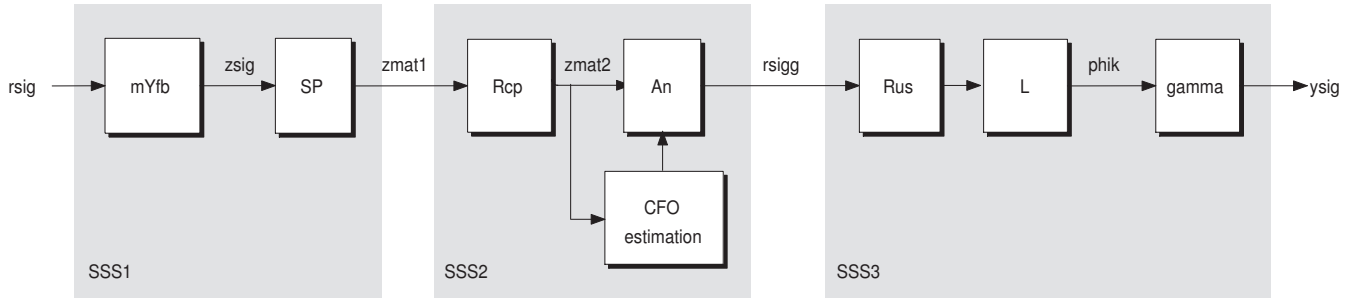

Fig. 1. The three-stage structure of the proposed blind multiuser channel-shortening receiver.

shortening performances can be obtained even for moderate-to-high SNR values. Thus, we choose $L_{\text{eff}} = L_{\text{cp}}$ and assume in our design that, for sufficiently high (but finite) SNR values, the perfect channel shortening condition (12) is satisfied by the MMOE shortener, i.e., $\mathbf{g}_k = \mathbf{H}_k^H \, \mathbf{\Sigma}_k^H \, \mathbf{f}_{\text{mmoe}} = [\mathbf{g}_{k,\text{win}}^T, \mathbf{0}_{L_{\text{g}}-L_{\text{cp}}}^T]^T \in \mathbb{C}^{L_{\text{g}}+1}$, where $\mathbf{g}_{k,\text{win}} \triangleq \mathbf{G}_{k,\text{win}} \boldsymbol{\gamma}$, with $\mathbf{G}_{k,\text{win}} \triangleq \mathbf{H}_{k,\text{win}}^H \, \mathbf{\Sigma}_k^H \, \mathbf{F}_{\text{mmoe}} \in \mathbb{C}^{(L_{\text{cp}}+1)\times Q(L_{\text{cp}}+1)}$. In such a case, the vector $\mathbf{z}(m) = \mathbf{F}_{\text{mmoe}}^H \, \overline{\mathbf{r}}(m) \in \mathbb{C}^{Q(L_{\text{cp}}+1)}$ can be written as

$$\mathbf{z}(m) = \sum_{k=1}^{K} e^{j\frac{2\pi}{M}\epsilon_k m} \, \mathbf{G}_{k,\text{win}}^H \, \overline{\mathbf{u}}_{k,\text{win}}(m) + \mathbf{v}(m) \qquad (16)$$

where $\mathbf{v}(m) \triangleq \mathbf{F}_{\text{mmoe}}^H \, \overline{\mathbf{w}}(m) \in \mathbb{C}^{Q(L_{\text{cp}}+1)}$. After carrying out the polyphase decomposition (with respect to P) of $y_{\text{mmoe}}(m) = \mathbf{z}^T(m)\boldsymbol{\gamma}^*$ and removing the CP to achieve IBI suppression, the TEQ output vector

$$\mathbf{y}_{\text{mmoe}}(n) \triangleq [y_{\text{mmoe}}(nP + L_{\text{cp}}), y_{\text{mmoe}}(nP + L_{\text{cp}} + 1), \ldots, y_{\text{mmoe}}(nP + P - 1)]^T \in \mathbb{C}^M$$

of IBI-free samples in the nth symbol period is given by $\mathbf{y}_{\text{mmoe}}(n) = \mathbf{Z}(n)\boldsymbol{\gamma}^*$, where

$$\mathbf{Z}(n) \triangleq [\mathbf{z}(nP+L_{\text{cp}}), \mathbf{z}(nP+L_{\text{cp}}+1), \ldots, \mathbf{z}(nP+P-1)]^T.$$

It is shown in Appendix C that $\mathbf{Z}(n)$ can be written as

$$\mathbf{Z}(n) = \mathbf{\Psi} \, \mathbf{A}(n) + \mathbf{V}(n) \qquad (17)$$

where, for $k \in \{1, 2, \ldots, K\}$ and $r \in \{0, 1, \ldots, K_{\text{m}} - 1\}$,

$$\begin{aligned}
\mathbf{\Psi} &\triangleq [\mathbf{\Psi}_1, \mathbf{\Psi}_2, \ldots, \mathbf{\Psi}_K] \in \mathbb{C}^{M \times KM_{\text{u}}} \\
\mathbf{\Psi}_k &\triangleq [\mathbf{\Psi}_k^{(0)}, \mathbf{\Psi}_k^{(1)}, \ldots, \mathbf{\Psi}_k^{(K_{\text{m}}-1)}]^T \in \mathbb{C}^{M \times M_{\text{u}}} \\
\mathbf{\Psi}_k^{(r)} &\triangleq K_{\text{m}}^{-1/2} \text{diag}\left[e^{j\frac{2\pi}{M} r M_{\text{u}}(\epsilon_k+\phi_k)}, \ldots, e^{j\frac{2\pi}{M}(rM_{\text{u}}+M_{\text{u}}-1)(\epsilon_k+\phi_k)}\right] \in \mathbb{C}^{M_{\text{u}} \times M_{\text{u}}} \\
\mathbf{A}(n) &\triangleq [\mathbf{a}_0(n), \mathbf{a}_1(n), \ldots, \mathbf{a}_{Q(L_{\text{cp}}+1)-1}(n)] \\
\mathbf{a}_i(n) &\triangleq [\{e^{j\frac{2\pi}{M}\epsilon_1(nP+L_{\text{cp}})} \, \widetilde{\boldsymbol{\mathcal{G}}}_{1,i} \, \mathbf{s}_1(n)\}^T, \ldots, \{e^{j\frac{2\pi}{M}\epsilon_K(nP+L_{\text{cp}})} \, \widetilde{\boldsymbol{\mathcal{G}}}_{K,i} \, \mathbf{s}_K(n)\}^T]^T \in \mathbb{C}^{KM_{\text{u}}} \\
\mathbf{V}(n) &\triangleq [\mathbf{v}(nP + L_{\text{cp}}), \ldots, \mathbf{v}(nP + P - 1)]^T
\end{aligned}$$

and $\widetilde{\boldsymbol{\mathcal{G}}}_{k,i} \in \mathbb{C}^{M_{\text{u}} \times M_{\text{u}}}$ is a circulant matrix with $[\{\mathbf{G}_{k,\text{win}}\}_{0,i}, \ldots, \{\mathbf{G}_{k,\text{win}}\}_{L_{\text{cp}},i} \, e^{j\frac{2\pi}{M}\phi_k L_{\text{cp}}}, \, 0, \ldots, 0]^H$ as first column, for $i \in \{0, 1, \ldots, Q(L_{\text{cp}} + 1) - 1\}$.

Due to the presence of the CFOs in (17), after performing DFT and subcarrier demapping, the K users are not orthogonal in the frequency domain, which highlights the need for CFO compensation.[4] Since the time-varying complex exponentials $\{e^{j\frac{2\pi}{M}\epsilon_k(nP+L_{\text{cp}})}\}_{k=1}^K$ in $\mathbf{A}(n)$ do not affect user separation, they can be compensated through simple per-user counter-rotation, performed after restoring orthogonality among uplink signals. Therefore, the key point is to restore orthogonality among users, by extracting from $\mathbf{Z}(n)$ an estimate $\widehat{\mathbf{A}}(n)$ of the matrix $\mathbf{A}(n)$, which separately gathers the contributions of all the active users. Since we have assumed that the CFOs have been previously estimated, the matrix $\mathbf{\Psi}$ is available in the following derivations. We resort to the least squares (LS) (also known as linear decorrelating detector in the multiuser detection literature) criterion to compute $\widehat{\mathbf{A}}(n)$. Under the assumption that the matrix $\mathbf{\Psi}$ is full-column rank, the minimum-norm LS estimate of $\mathbf{A}(n)$ is given by

$$\widehat{\mathbf{A}}(n) = \mathbf{\Psi}^\dagger \, \mathbf{Z}(n) = \mathbf{A}(n) + \mathbf{\Psi}^\dagger \, \mathbf{V}(n) \qquad (18)$$

where $\mathbf{\Psi}^\dagger = (\mathbf{\Psi}^H \, \mathbf{\Psi})^{-1} \mathbf{\Psi}^H$ is the Moore-Penrose inverse of $\mathbf{\Psi}$, which completely suppresses the MAI produced by the CFOs in the ideal case of perfectly estimated CFOs. The full-column rank property of $\mathbf{\Psi}$ is implicitly assumed in [7] without proving it: it is demonstrated in Appendix D that $\mathbf{\Psi}$ is full-column rank, provided that $e^{j\frac{2\pi}{K_{\text{m}}}(\epsilon_1+\phi_1)} \neq e^{j\frac{2\pi}{K_{\text{m}}}(\epsilon_2+\phi_2)} \neq \cdots \neq e^{j\frac{2\pi}{K_{\text{m}}}(\epsilon_K+\phi_K)}$, i.e., $(\epsilon_{k_1}+\phi_{k_1})-(\epsilon_{k_2}+\phi_{k_2}) \neq i\,K_{\text{m}}$, for any $k_1 \neq k_2 \in \{1, 2, \ldots, K\}$ and $\forall i \in \mathbb{Z}$. Remembering that the CFOs satisfy $|\epsilon_k| < 1/2$, which implies that $|\epsilon_{k_1} - \epsilon_{k_2}| < 1$, and noting that $\phi_{k_1} - \phi_{k_2} \in \{-K_{\text{m}}+1, \ldots, K_{\text{m}}-1\} - \{0\}$, it can be inferred that the previous condition is always satisfied.[5]

In the presence of additive noise, perfect CFO compensation comes at the price of a certain noise amplification. To alleviate such a problem, a successive interference cancellation algorithm has been devised in [7], which however may be plagued by error propagation and, moreover, it is particularly sensitive to the adopted ordering of the active users. In the following subsection, we will propose a completely different approach, which exploits the available degrees of freedom represented by

[4]The matrix $\widetilde{\boldsymbol{\mathcal{G}}}_{k,i}$ also depends on the CFO ϵ_k, since $\mathbf{G}_{k,\text{win}}$ is a function of ϵ_k through $\mathbf{\Sigma}_k$. However, such a dependence does not affect user separability, since it is automatically compensated by frequency-domain channel equalization.

[5]It can also be inferred that $\mathbf{\Psi}$ begins to lose rank when the distance between the residual CFOs approaches unity, e.g., when $\epsilon_{k_1} = -\epsilon_{k_2} = \pm 1/2$, which occurs with probability zero in practical cases.

the constraint vector $\boldsymbol{\gamma}$ in (13), to perform blind maximization of the SNR for each user in the frequency domain.

C. Blind per-user SNR maximization

We assume that IBI has been removed and the CFOs have been perfectly compensated. Thus, having restored orthogonality among users, user separation can be achieved by picking out the $M_{\rm u} \times Q(L_{\rm cp}+1)$-dimensional sub-matrices of $\widehat{\mathbf{A}}(n)$. The resulting kth-user data matrix $\widehat{\mathbf{A}}_k(n) \in \mathbb{C}^{M_{\rm u} \times Q(L_{\rm cp}+1)}$, for $k \in \{1,2,\ldots,K\}$, can be expressed as

$$\begin{aligned}\widehat{\mathbf{A}}_k(n) &= \mathbf{R}_k\, \widehat{\mathbf{A}}(n) \\ &= e^{j\frac{2\pi}{M}\epsilon_k(nP+L_{\rm cp})} \Big[\widetilde{\boldsymbol{\mathcal{G}}}_{k,0}\, \mathbf{s}_k(n), \widetilde{\boldsymbol{\mathcal{G}}}_{k,1}\, \mathbf{s}_k(n), \ldots, \\ &\quad \widetilde{\boldsymbol{\mathcal{G}}}_{k,Q(L_{\rm cp}+1)-1}\, \mathbf{s}_k(n)\Big] + \mathbf{R}_k\, \boldsymbol{\Psi}^\dagger\, \mathbf{V}(n) \qquad (19)\end{aligned}$$

where $\mathbf{R}_k \triangleq [\mathbf{O}_{(k-1)M_{\rm u}\times M_{\rm u}}, \mathbf{I}_{M_{\rm u}}, \mathbf{O}_{(K-k)M_{\rm u}\times M_{\rm u}}]$ is the extraction matrix. By recalling the eigenstructure properties of circulant matrices, we write $\widetilde{\boldsymbol{\mathcal{G}}}_{k,i} = \mathbf{W}_{\rm dft}^H\, \boldsymbol{\Lambda}_{k,i}\, \mathbf{W}_{\rm dft}$, where $\boldsymbol{\Lambda}_{k,i} \triangleq {\rm diag}(\boldsymbol{\lambda}_{k,i}) \in \mathbb{C}^{M_{\rm u}\times M_{\rm u}}$ and

$$\boldsymbol{\lambda}_{k,i} \triangleq {M_{\rm u}}^{1/2}\, \mathbf{W}_{\rm dft}\, \mathbf{C}\, \mathbf{E}_k\, [\{\mathbf{G}_{k,\rm win}\}_{0,i}, \ldots, \{\mathbf{G}_{k,\rm win}\}_{L_{\rm cp},i}]^H$$

for $i \in \{0,1,\ldots,Q(L_{\rm cp}+1)-1\}$, with

$$\begin{aligned}\mathbf{C} &\triangleq [\mathbf{I}_{L_{\rm cp}+1}, \mathbf{O}_{(L_{\rm cp}+1)\times(M_{\rm u}-L_{\rm cp}-1)}]^T \in \mathbb{R}^{M_{\rm u}\times(L_{\rm cp}+1)} \\ \mathbf{E}_k &\triangleq {\rm diag}(1, e^{-j\frac{2\pi}{M}\phi_k}, \ldots, e^{-j\frac{2\pi}{M}\phi_k L_{\rm cp}}) \in \mathbb{C}^{L_{\rm cp}+1}\,. \qquad (20)\end{aligned}$$

Thus, after DFT, one has

$$\begin{aligned}\mathbf{Q}_k(n) &\triangleq \mathbf{W}_{\rm dft}\, \widehat{\mathbf{A}}_k(n) \\ &= M_{\rm u}^{1/2} e^{j\frac{2\pi}{M}\epsilon_k(nP+L_{\rm cp})}\, \widetilde{\mathbf{S}}_k(n)\, \mathbf{W}_{\rm dft}\, \mathbf{C}\, \mathbf{E}_k\, \mathbf{G}_{k,\rm win}^* \\ &\quad + \mathbf{W}_{\rm dft}\, \mathbf{N}_k(n)\, \mathbf{F}_{\rm mmoe}^* \\ &= M_{\rm u}^{1/2} e^{j\frac{2\pi}{M}\epsilon_k(nP+L_{\rm cp})}\, \boldsymbol{\Lambda}_k\, \widetilde{\mathbf{s}}_k(n) \\ &\quad + \mathbf{W}_{\rm dft}\, \mathbf{N}_k(n)\, \mathbf{F}_{\rm mmoe}^* \qquad (21)\end{aligned}$$

with

$$\begin{aligned}&\widetilde{\mathbf{S}}_k(n) \triangleq {\rm diag}[\widetilde{\mathbf{s}}_k(n)] \in \mathbb{C}^{M_{\rm u}\times M_{\rm u}} \\ &\mathbf{N}_k(n) \triangleq \mathbf{R}_k \boldsymbol{\Psi}^\dagger\, \overline{\mathbf{W}}(n) \in \mathbb{C}^{M_{\rm u}\times Q(L_{\rm e}+1)} \\ &\overline{\mathbf{W}}(n) \triangleq [\overline{\mathbf{w}}(nP+L_{\rm cp}), \ldots, \overline{\mathbf{w}}(nP+P-1)]^T \in \mathbb{C}^{M\times Q(L_{\rm e}+1)} \\ &\boldsymbol{\Lambda}_k \triangleq {\rm diag}(\mathbf{W}_{\rm dft}\, \mathbf{C}\, \mathbf{E}_k\, \mathbf{G}_{k,\rm win}^*) \in \mathbb{C}^{M_{\rm u}\times M_{\rm u}}\,. \qquad (22)\end{aligned}$$

To take into account the constraint vector $\boldsymbol{\gamma}$, observe that the cascade of CFO compensation, user separation, and DFT can be equivalently seen as a linear transformation of the TEQ output vector $\mathbf{y}_{\rm mmoe}(n) = \mathbf{Z}(n)\, \boldsymbol{\gamma}^*$, which allows one to write the frequency-domain vector $\widehat{\mathbf{q}}_k(n)$ as

$$\widehat{\mathbf{q}}_k(n) \triangleq \mathbf{W}_{\rm dft}\, \mathbf{R}_k\, \boldsymbol{\Psi}^\dagger\, \mathbf{y}_{\rm mmoe}(n) = \mathbf{Q}_k(n)\, \boldsymbol{\gamma}^* \qquad (23)$$

where $\mathbf{Q}_k(n) = \mathbf{W}_{\rm dft}\, \mathbf{R}_k\, \boldsymbol{\Psi}^\dagger\, \mathbf{Z}(n)$ is given by (21). Therefore, the SNR associated[6] with (23) is

$$\begin{aligned}{\rm SNR}_k &\triangleq \frac{\mathbb{E}\left[\left\| M_{\rm u}^{1/2}\, \widetilde{\mathbf{S}}_k(n)\, \mathbf{W}_{\rm dft}\, \mathbf{C}\, \mathbf{E}_k\, \mathbf{G}_{k,\rm win}^*\, \boldsymbol{\gamma}^* \right\|^2\right]}{\mathbb{E}\left[\left\| \mathbf{W}_{\rm dft}\, \mathbf{N}_k(n)\, \mathbf{F}_{\rm mmoe}^*\, \boldsymbol{\gamma}^* \right\|^2\right]} \\ &= \frac{\boldsymbol{\gamma}^H\, \mathbf{R}_{\mathbf{Q}_k\mathbf{Q}_k}^*\, \boldsymbol{\gamma}}{\boldsymbol{\gamma}^H\, \mathbf{F}_{\rm mmoe}^H\, \mathbf{R}_{\mathbf{N}_k\mathbf{N}_k}^*\, \mathbf{F}_{\rm mmoe}\, \boldsymbol{\gamma}} - 1 \qquad (24)\end{aligned}$$

where

$$\begin{aligned}\mathbf{R}_{\mathbf{Q}_k\mathbf{Q}_k} &\triangleq \mathbb{E}[\mathbf{Q}_k^H(n)\, \mathbf{Q}_k(n)] = \sigma_s^2\, M_{\rm u}\, \mathbf{G}_{k,\rm win}^T\, \mathbf{G}_{k,\rm win}^* \\ &\quad + \mathbf{F}_{\rm mmoe}^T\, \mathbf{R}_{\mathbf{N}_k\mathbf{N}_k}\, \mathbf{F}_{\rm mmoe}^* \in \mathbb{C}^{Q(L_{\rm cp}+1)\times Q(L_{\rm cp}+1)}\end{aligned}$$

with $\mathbf{R}_{\mathbf{N}_k\mathbf{N}_k} \triangleq \mathbb{E}[\mathbf{N}_k^H(n)\, \mathbf{N}_k(n)] \in \mathbb{C}^{Q(L_{\rm e}+1)\times Q(L_{\rm e}+1)}$. In Appendix E, it is proven that $\mathbf{R}_{\mathbf{N}_k\mathbf{N}_k}$ is a scaled identity matrix, thus maximizing (24) with respect to $\boldsymbol{\gamma}$ leads to

$$\begin{aligned}\boldsymbol{\gamma}_{k,\rm opt} = \arg\max_{\boldsymbol{\gamma}} &\left\{\boldsymbol{\gamma}^H\, \mathbf{R}_{\mathbf{Q}_k\mathbf{Q}_k}^*\, \boldsymbol{\gamma}\right\} \\ &\text{subject to} \quad \boldsymbol{\gamma}^H\, \mathbf{F}_{\rm mmoe}^H\, \mathbf{F}_{\rm mmoe}\, \boldsymbol{\gamma} = 1 \qquad (25)\end{aligned}$$

whose solution depends on k and can be expressed (see, e.g., [24]) as $\boldsymbol{\gamma}_{k,\rm opt} = \mathbf{R}_{\rm mmoe}^{-1}\, \widetilde{\boldsymbol{\gamma}}_{k,\max}$, where $\widetilde{\boldsymbol{\gamma}}_{k,\max}$ is the eigenvector associated with the largest eigenvalue of matrix $(\mathbf{R}_{\rm mmoe}^{-1})^H\, \mathbf{R}_{\mathbf{Q}_k\mathbf{Q}_k}^*\, \mathbf{R}_{\rm mmoe}^{-1}$, and $\mathbf{F}_{\rm mmoe} = \mathbf{Q}_{\rm mmoe}\, \mathbf{R}_{\rm mmoe}$ is the QR decomposition of $\mathbf{F}_{\rm mmoe}$, with $\mathbf{R}_{\rm mmoe} \in \mathbb{C}^{Q(L_{\rm cp}+1)\times Q(L_{\rm cp}+1)}$ being a nonsingular upper triangular matrix and $\mathbf{Q}_{\rm mmoe} \in \mathbb{C}^{Q(L_{\rm e}+1)\times Q(L_{\rm cp}+1)}$ being a semi-unitary matrix, i.e., $\mathbf{Q}_{\rm mmoe}^H \mathbf{Q}_{\rm mmoe} = \mathbf{I}_{Q(L_{\rm cp}+1)}$. The vector $\boldsymbol{\gamma}_{k,\rm opt}$ can be consistently estimated from the received data either in batch or adaptive mode [24]. It is worthwhile to note that the resulting receiver admits the *three-stage* structure depicted in Fig. 1. A summary of the proposed algorithm and its computational complexity [expressed in floating point operations (flops)] is reported in Tab. I for $L_{\rm eff} = L_{\rm cp}$.

To recover from $\widehat{\mathbf{q}}_k(n)$ the kth-user symbol block $\mathbf{s}_k(n)$, we resort to the minimum mean-square error (MMSE) estimator, given by

$$\begin{aligned}\widehat{\mathbf{s}}_k(n) = \sigma_s^2\, e^{-j\frac{2\pi}{M}\epsilon_k(nP+L_{\rm cp})}\, \mathbf{W}_{\rm dft}^H\, \boldsymbol{\Lambda}_k^* \\ \cdot \left(\sigma_s^2\, \boldsymbol{\Lambda}_k\, \boldsymbol{\Lambda}_k^* + \sigma_w^2\, |\mu_k|^2\, \mathbf{I}_{M_{\rm u}}\right)^{-1} \widehat{\mathbf{q}}_k(n) \qquad (26)\end{aligned}$$

where the knowledge of $\boldsymbol{\Lambda}_k^*$ (assumed to be non singular) can be obtained by estimating the shortened channel vector $\mathbf{g}_{k,\rm win}$ by means of conventional blind or training-based channel estimators, whereas $\mu_k \triangleq K_{\rm m}^{-1/2} \sum_{\ell=1}^K \mu_{k,\ell}$, with $\mu_{k,\ell} \triangleq \{(\boldsymbol{\Psi}^H\boldsymbol{\Psi})^{-1}\}_{(k-1)M_{\rm u}+1,(\ell-1)M_{\rm u}+1}$ (see also Appendix E).[7] Each entry of $\widehat{\mathbf{s}}_k(n)$ is finally quantized to the nearest (in Euclidean distance) information symbol, to form the estimate of the corresponding entry of $\mathbf{s}_k(n)$.

[6] Under our assumptions, the only disturbance in (23) is thermal noise, which allows one to devise a blind maximum-SNR criterion, instead of a more complicated and non-blind maximum signal-to-interference-plus-noise (SINR) one.

[7] In practice, only a reliable estimate $\widehat{\epsilon}_k$ of the CFO ϵ_k is available to compensate for the time-varying exponential $e^{j\frac{2\pi}{M}\epsilon_k(nP+L_{\rm cp})}$. In this case, the task of eliminating the residual factor $e^{j\frac{2\pi}{M}(\epsilon_k-\widehat{\epsilon}_k)(nP+L_{\rm cp})}$ is assigned to the phase recovery circuit [39].

TABLE I
SUMMARY AND COMPLEXITY OF THE PROPOSED ALGORITHM.

- **Blind multiuser MMOE channel shortening**:
  - multiuser MMOE channel shortening: $\mathbf{z}(m) \triangleq \mathbf{F}_{\text{mmoe}}^H \, \overline{\mathbf{r}}(m) \in \mathbb{C}^{Q(L_{\text{cp}}+1)}$, with $\mathbf{F}_{\text{mmoe}}$ given by (14) or (34);
  - serial-to-parallel conversion: $\widetilde{\mathbf{Z}}(n) \triangleq [\mathbf{z}(nP), \mathbf{z}(nP+1), \ldots, \mathbf{z}(nP+P-1)]^T \in \mathbb{C}^{P \times Q(L_{\text{cp}}+1)}$;
  - complexity dominated by calculation of $\mathbf{F}_{\text{mmoe}}$, requiring $\mathcal{O}[Q^3(L_{\text{e}}-L_{\text{cp}})^3)]$ flops when expressed by (34).
- **Blind multiuser CFO compensation**:
  - CP removal: $\mathbf{Z}(n) \triangleq \mathbf{R}_{\text{cp}} \, \widetilde{\mathbf{Z}}(n) \in \mathbb{C}^{M \times Q(L_{\text{cp}}+1)}$, with $\mathbf{R}_{\text{cp}} \triangleq [\mathbf{O}_{M \times L_{\text{cp}}}, \mathbf{I}_M] \in \mathbb{R}^{M \times P}$;
  - CFO compensation: $\widehat{\mathbf{A}}(n) \triangleq \mathbf{\Psi}^{\dagger} \, \mathbf{Z}(n) \in \mathbb{C}^{KM_{\text{u}} \times Q(L_{\text{cp}}+1)}$;
  - complexity dominated by calculation of $\mathbf{\Psi}^{\dagger}$, requiring $\mathcal{O}(K^3 M_{\text{u}}^3)$ flops.
- **Blind per-user SNR maximization**:
  - kth user extraction and DFT: $\mathbf{Q}_k(n) \triangleq \mathbf{W}_{\text{dft}} \, \mathbf{R}_k \, \widehat{\mathbf{A}}(n) \in \mathbb{C}^{M_u \times Q(L_{\text{cp}}+1)}$;
  - per-user maximum-SNR filtering: $\widehat{\mathbf{q}}_k(n) \triangleq \mathbf{Q}_k(n) \, \boldsymbol{\gamma}^* \in \mathbb{C}^{M_u}$, with $\boldsymbol{\gamma} = \boldsymbol{\gamma}_{k,\text{opt}}$ given by (25);
  - complexity dominated by calculation of the dominant eigenvector in (25), requiring $\mathcal{O}[Q^3(L_{\text{cp}}+1)^2(L_{\text{e}}+1)]$ flops needed to evaluate the QR decomposition of $\mathbf{F}_{\text{mmoe}}$.

IV. SIMULATION RESULTS

We present in this section the results of Monte Carlo computer simulations, aimed at assessing the performance of the proposed blind MMOE receiver, in comparison with the blind receiver of [31], which employs the carrier nulling algorithm (CNA), and the non-blind MMSE method of [15], which requires *a priori* knowledge of the *long* (i.e., before channel shortening) CIR; both receivers were adapted to work in the considered SC-IFDMA scenario. In addition, as a reference, we report the performance of the receiver without channel shortening (referred to as "w/o TEQ").

Unless otherwise specified, the SC-IFDMA uplink works with 2x oversampling ($N_{\text{c}} = 2$) and employs a total of $M = 64$ QPSK-modulated subcarriers, with a CP of length $L_{\text{cp}} = 4$. For each $k \in \{1, 2, \ldots, K\}$ and $\ell \in \{0, 1, \ldots, L_k\}$, the elements of the channel vector $\mathbf{h}_k(\ell)$ are randomly generated in each Monte Carlo trial as independent and identically distributed (i.i.d.) circularly symmetric complex Gaussian random variables with zero mean and variance $\sigma_h^2(\ell)$, with $\mathbf{h}_{k_1}(\ell_1)$ and $\mathbf{h}_{k_2}(\ell_2)$ statistically independent of each other for $k_1 \neq k_2$ or $\ell_1 \neq \ell_2$. We assumed an exponential power-delay profile model, with $\sigma_h^2(\ell) = \sigma_h^2(0) \, \exp(-0.1\,\ell)$, for $\ell \in \{0, 1, \ldots, L_k\}$, where $\sigma_h^2(0)$ is chosen to ensure a unit average energy for $\mathbf{h}_k(\ell)$, and we set $\theta_k = 0$ and (unless otherwise specified) $L_k = L_{\max} = 6$. The additive noise vector $\mathbf{w}(m)$ is modeled as a zero-mean white complex circularly symmetric Gaussian vector. In all experiments, the first user (i.e., $k = 1$) is chosen as the desired one and, according to (5), its received average SNR is defined as $\text{SNR} \triangleq (\sigma_w^2 Q)^{-1} \, \mathbb{E}[\| \sum_{\ell=0}^{L_{\max}} \mathbf{h}_1(\ell) u_1(m-\ell) \|^2]$.

The first figure of merit computed in our simulations is the average shortening SINR (ASSINR) [24] at the output of the TEQs, which is defined [see (10) and (11)] as

$$\text{ASSINR} \triangleq \frac{\mathbb{E}\left[\left|\mathbf{g}_{1,\text{win}}^H \, \overline{\mathbf{u}}_{1,\text{win}}(m)\right|^2\right]}{\mathbb{E}\left[\left|\mathbf{g}_{1,\text{wall}}^H \, \overline{\mathbf{u}}_{1,\text{wall}}(m) + v(m)\right|^2\right]} \,. \tag{27}$$

and represents a measure of their channel shortening capabilities.[8] To assess the overall performance of the receivers, we evaluated the average BER (ABER) at their output, which is the average of the BERs measured over the M_{u} subcarriers employed by the desired user.

Both ASSINR and ABER values are obtained by averaging the results over 3000 SC-IFDMA symbols and 1000 Monte Carlo trials, assuming for data demodulation exact knowledge of the shortened channel after TEQ, which can be achieved by standard channel estimation techniques.

The proposed MMOE is implemented in both its exact (referred to as "ex.") and data-dependent (referred to as "est.") versions: in the first implementation, we assumed perfect knowledge of the covariance matrix $\mathbf{R}_{\overline{\mathbf{r}}\overline{\mathbf{r}}}$ needed for the synthesis of the channel shortener; whereas, in the second one, the matrix $\mathbf{R}_{\overline{\mathbf{r}}\overline{\mathbf{r}}}$ is estimated in batch mode on the basis of a sample-size of $K_s = 40$ (unless otherwise specified) SC-IFDMA symbols. The CNA TEQ, which maximizes a cost function that does not admit a closed-form expression, is implemented in a blind data-estimated manner, as described in [31], utilizing again $K_s = 40$ SC-IFDMA symbols. Finally, the MMSE and the "w/o TEQ" receivers are implemented exactly in all the experiments.

A. Channel shortening performance

In this subsection, we focus on the ASSINR performances of the TEQs under comparison. We considered a system with $K = 2$ users, each employing $M_{\text{u}} = 32$ subcarriers, a BS equipped with $N_{\text{r}} = 3$ antennas, and we set the TEQ order to $L_{\text{e}} = 10$. Moreover, we considered two scenarios, either when no CFO is present (i.e., $\epsilon_1 = \epsilon_2 = 0$), or when the CFOs are chosen as $(\epsilon_1, \epsilon_2) = (0.20, -0.32)$.

Figs. 2 and 3, which report the ASSINR as a function of SNR in the two CFO scenarios, show that, since $L_{\text{cp}} < L_{\max}$, the performances of the "w/o TEQ" receiver are completely unsatisfactory over the entire range of SNR. In contrast, the proposed MMOE, both in its exact and data-estimated versions, exhibits satisfactory performances, which are almost

[8] It is worthwhile to note that, for the proposed MMOE, the calculation of ASSINR includes the effects of optimization of $\boldsymbol{\gamma}$ carried out in the third stage.

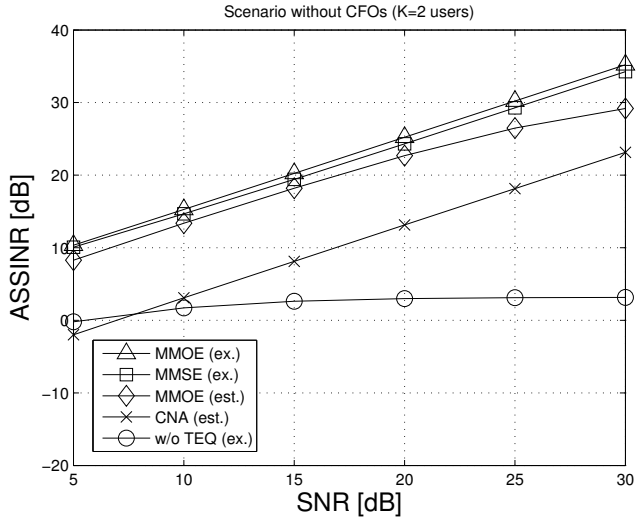

Fig. 2. Average shortening SINR versus SNR ($K = 2$ users, scenario without CFOs).

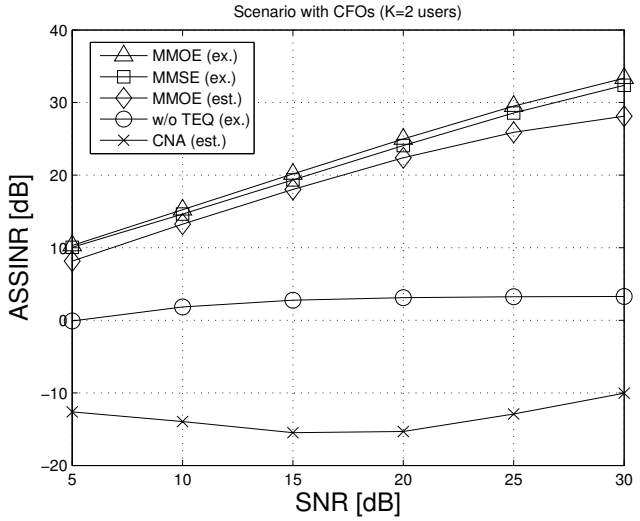

Fig. 3. Average shortening SINR versus SNR ($K = 2$ users, scenario with CFOs).

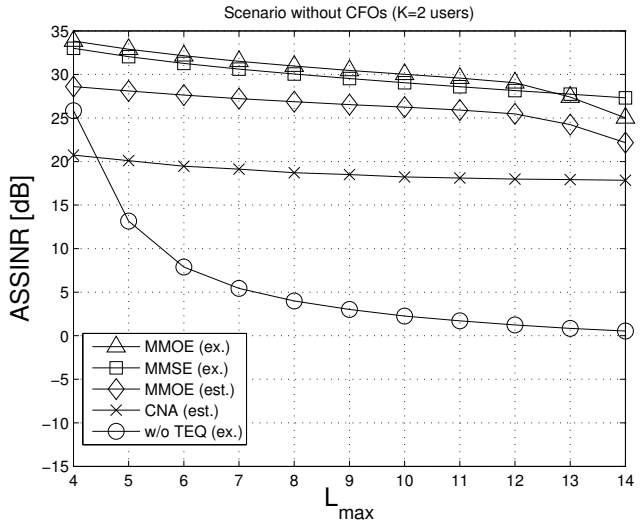

Fig. 4. Average shortening SINR versus $L_{\max}$ ($K = 2$ users, scenario without CFOs).

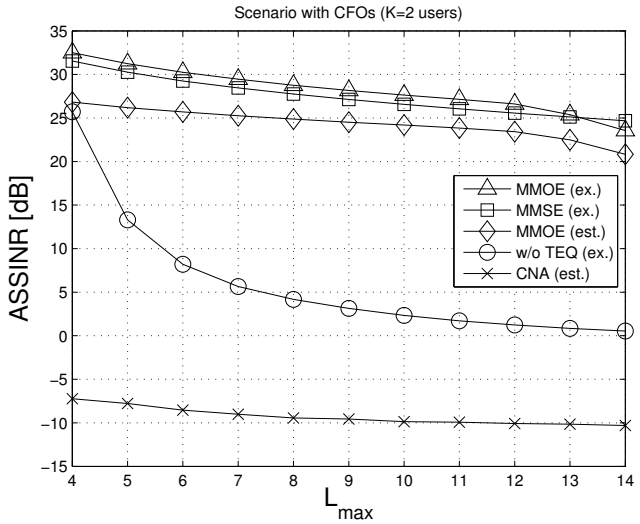

Fig. 5. Average shortening SINR versus $L_{\max}$ ($K = 2$ users, scenario with CFOs).

insensitive to the presence of the CFOs. In particular, in both CFO scenarios, the MMOE performs comparably to the non-blind MMSE TEQ, exhibiting even a slight performance advantage when implemented exactly: this behavior, which seems counterintuitive at first sight, can be explained by noting that, while the MMSE exploits all its degrees of freedom to jointly shorten the CIRs *and* suppress ICI and MAI, the MMOE employs its degrees of freedom only to shorten the CIRs, since ICI/MAI suppression is assured, after CP removal, by restoring subcarrier orthogonality. Compared to its exact version, the data-estimated MMOE pays a penalty of about 5 dB for high SNR values in both CFO scenarios; this behavior is due to the well-studied performance saturation effect [40] which, however, can be reduced (if needed) by properly increasing the sample-size K_s. As regards the comparison with the blind CNA shortener, in the absence of CFOs (Fig 2), the data-estimated MMOE provides a 10-dB gain over almost the entire SNR range, which is largely due to the per-user SNR maximization carried out in its third stage;[9] instead, in the presence of CFOs (Fig 3), the CNA performance is completely unsatisfactory, due to the lack of a fine frequency synchronization step to be performed before channel shortening.

Figs. 4 and 5 report the ASSINR of the considered TEQs as a function of the maximum channel order $L_{\max} \in \{4, \ldots, 13\}$, in the two CFO scenarios and for a fixed SNR $= 25$ dB. Note that, when $L_{\max} \geq 13$, condition (15) is violated, i.e., perfect channel shortening is not ensured for the proposed MMOE even in the absence of noise; on the other hand, when $L_{\max} = L_{\text{cp}} = 4$, CP removal is capable of completely suppressing IBI: only in this case the ASSINR of the "w/o TEQ" receiver assumes acceptable values in both CFO scenarios, whose performances are however worse than those of the proposed receiver, due to the per-user SNR maximization carried out in its third stage. It is noteworthy that the performance of the proposed MMOE, both in its exact and

[9]Simulation results not reported here show indeed that SNR maximization in the third stage accounts for an ASSINR improvement of about 10 dB in the considered scenario.

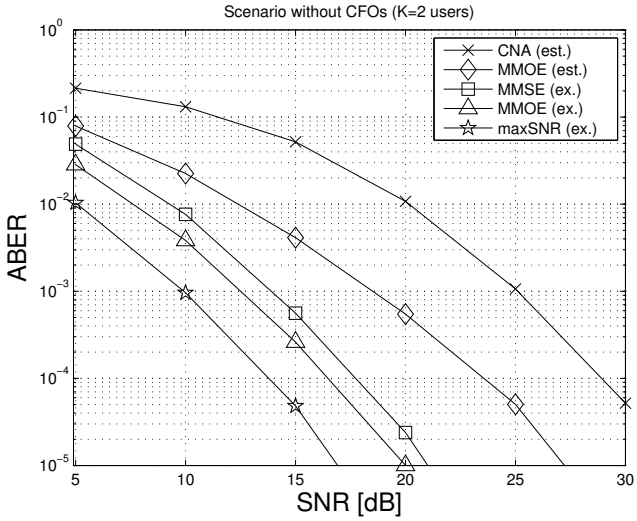

Fig. 6. Average BER versus SNR ($K = 2$ users, scenario without CFOs).

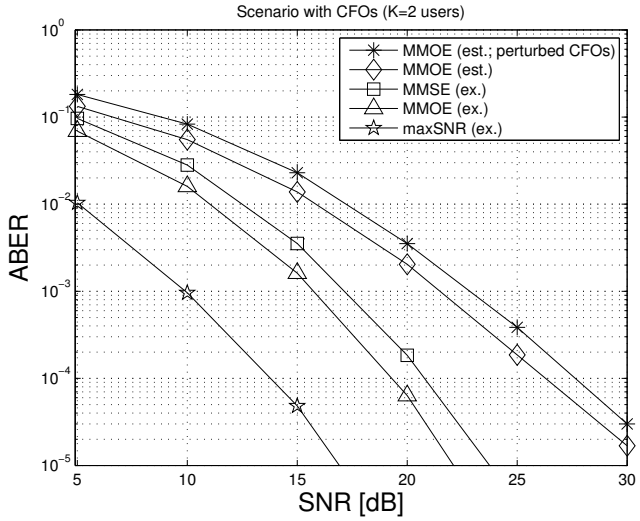

Fig. 7. Average BER versus SNR ($K = 2$ users, scenario with CFOs).

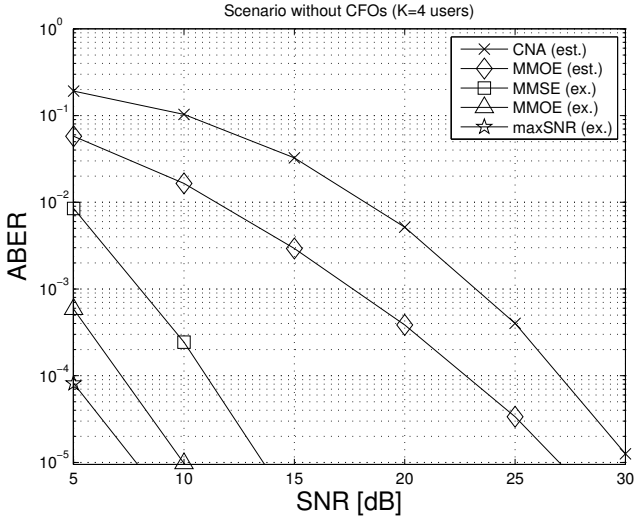

Fig. 8. Average BER versus SNR ($K = 4$ users, scenario without CFOs).

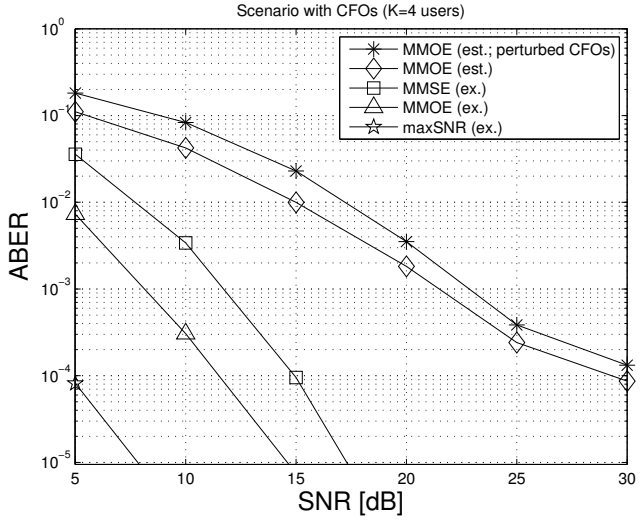

Fig. 9. Average BER versus SNR ($K = 4$ users, scenario with CFOs).

data-estimated versions, gracefully degrades as $L_{\max}$ increases, providing again large performance gains over the CNA one, which shows poor performances in the presence of CFOs (Fig.5). Moreover, the exact version of the MMOE performs again comparably to (or even better than) the non-blind MMSE one in both CFO scenarios and over the range of $L_{\max}$ values for which condition (15) is fulfilled, while its data-estimated counterpart pays an acceptable performance loss, which can be further reduced by increasing the sample-size K_s.

B. Overall receiver performances

In this subsection, we report the ABER performances of the complete receivers (encompassing the channel shortening algorithm, the CFO compensation procedure, and the symbol detector) as a function of SNR, with the exclusion of the "w/o TEQ" receiver, whose performance, being dominated by IBI, is completely unsatisfactory, as shown by simulations of Subsection IV-A.

Moreover, as a performance benchmark, we consider the non-blind receiver (labeled as "maxSNR" in the plots), which maximizes the per-user SNR in the frequency domain (before channel estimation and symbol detection): this receiver is implemented exactly and operates in an idealized scenario, wherein the channel order is equal to the CP length and no CFO is present.

We considered two SC-IFDMA systems, with $K = 2$ and $K = 4$ users: for the first one (results in Figs. 6 and 7), we considered the same setting of Subsection IV-A, i.e., $M_{\rm u} = 32$, $N_{\rm r} = 3$, and $L_{\rm e} = 10$; whereas for the second one (Figs. 8 and 9), we set $M_{\rm u} = 16$, $N_{\rm r} = 8$, and $L_{\rm e} = 7$. As in Subsection IV-A, we considered the two scenarios when no CFO is present or when the uplink signals are affected by CFOs: in the latter case, the CFOs are orderly chosen in the set $(0.20, -0.32, -0.18, 0.25)$. Moreover, we report the ABER performance of the proposed data-estimated MMOE not only when the CFOs are exactly known at the second stage, but also when the true CFO values are affected by a random perturbation: specifically, to perform LS compensation in (18), we replace ϵ_k in the construction of $\mathbf{\Psi}$ with $\widehat{\epsilon}_k = \epsilon_k + \Delta\epsilon_k$, for $k \in \{1, 2, \ldots, K\}$, where $\Delta\epsilon_1, \Delta\epsilon_2, \ldots, \Delta\epsilon_K$ are i.i.d.

(real) Gaussian random variables with zero mean and variance equal to the corresponding Cramér-Rao lower bound for CFO estimation, which is evaluated similarly to [41].

Simulation results confirm that, when no CFO is present (Figs. 6 and 8), the per-user SNR maximization carried out in the third stage allows both versions of the MMOE receiver to largely outperforms the CNA one.[10] Moreover, the exact version of the proposed MMOE receiver noticeably outperforms the non-blind MMSE one in both CFO scenarios, while its data-estimated counterpart pays only a moderate performance penalty, which grows when the number of users increases from $K = 2$ to $K = 4$: this behavior is mainly due to the marked increase of the size of the covariance matrix $\mathbf{R}_{\overline{\mathbf{r}}\overline{\mathbf{r}}}$ to be estimated (from 66×66 for $K = 2$ to 128×128 for $K = 4$), which would require a corresponding increase in sample-size to keep the estimation accuracy unchanged. It is remarkable that in all simulations the proposed MMOE pays only a reasonable performance loss with respect to the "maxSNR" ideal benchmark, which operates with a shortened channel and without CFOs. With reference to the scenarios with CFOs (Figs. 7 and 9), it is interesting to observe that CFO perturbations have a moderate impact on the performance of the proposed data-estimated MMOE.

In the last experiment, we assess the performance of the proposed data-estimated MMOE receivers in the scenario where the number of users ranges from $K = 1$ to $K = 5$, the CFOs are orderly chosen in the set $\{0.20, -0.32, -0.18, 0.25, -0.09\}$, and the number of subcarriers is $M_{\mathrm{u}} = \lfloor M/K \rfloor$.[11] Fig. 10 reports the ABER performance versus K for SNR = 30 dB, $N_{\mathrm{c}} = 3$, $N_{\mathrm{r}} = 12$, $L_{\mathrm{e}} = 5$, and $K_s = 20$ SC-IFDMA symbols. Results show that the overall performances of the considered receivers gracefully degrade as the number of users increases, exhibiting moreover a slightly larger sensitivity to CFO estimation errors.

V. Conclusions

In this paper, we proposed a receiver for the uplink of a SC-IFDMA system, where user signals are affected by TOs and CFOs and the quasi-synchronous assumption is violated, i.e., the CP length is insufficient to compensate for TOs and multipath channel dispersion. The proposed receiver is composed of three stages: (i) a constrained MMOE-based blind multiuser channel shortener, which can be entirely estimated from the received data, whose channel shortening capabilities are not impaired by the presence of CFOs; (ii) a LS compensator of the CFOs; (iii) a per-user blind maximum SNR-based detector. The proposed receiver outperforms existing solutions, based either on non-blind or blind channel shortening algorithms, by additionally showing a remarkable robustness against CFO estimation errors. An interesting issue to be investigated is how to take into account in our blind design the effects of transmitter and/or receiver I/Q imbalance.

[10] We did not report the performance of the CNA receiver in the presence of CFOs, since it does not work at all (see simulation results of Subsection IV-A).

[11] In this experiment, the remaining $M - M_{\mathrm{u}}K$ subcarriers are unmodulated.

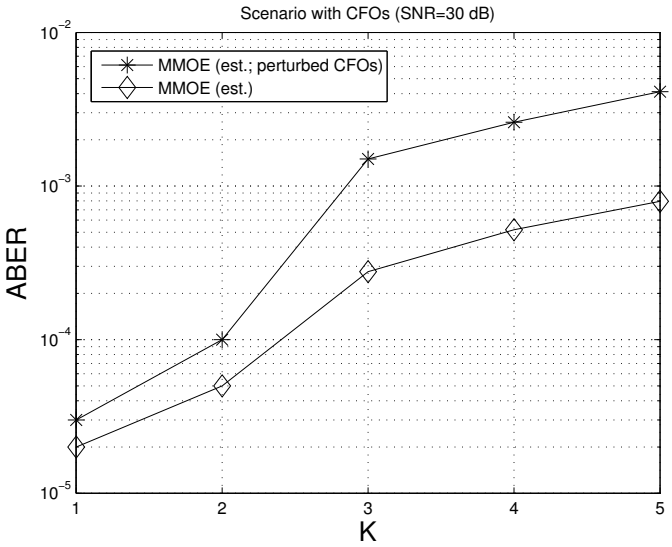

Fig. 10. Average BER versus K (SNR = 30 dB, scenario with CFOs).

Appendix A
Properties of the covariance matrix $\mathbf{R}_{\overline{\mathbf{r}}\overline{\mathbf{r}}}$

From (6), it results that

$$\mathbf{R}_{\overline{\mathbf{r}}\overline{\mathbf{r}}}(m) = \sum_{k=1}^{K} \mathbf{\Sigma}_k \, \mathbf{H}_k \, \mathbf{R}_{\overline{\mathbf{u}}_k\overline{\mathbf{u}}_k}(m) \, \mathbf{H}_k^H \, \mathbf{\Sigma}_k^H + \sigma_w^2 \, \mathbf{I}_{Q(L_{\mathrm{e}}+1)} \tag{28}$$

where $\mathbf{R}_{\overline{\mathbf{u}}_k\overline{\mathbf{u}}_k}(m) \triangleq \mathbb{E}[\overline{\mathbf{u}}_k(m)\,\overline{\mathbf{u}}_k^H(m)] \in \mathbb{C}^{(L_g+1)\times(L_g+1)}$ is the covariance matrix of $\overline{\mathbf{u}}_k(m)$, for $k \in \{1, 2, \ldots, K\}$, whose elements are $\{\mathbf{R}_{\overline{\mathbf{u}}_k\overline{\mathbf{u}}_k}(m)\}_{i_1 i_2} = R_{u_k u_k}(m - i_1, i_2 - i_1)$, for $0 \le i_1, i_2 \le L_{\mathrm{g}} < P$, where

$$R_{u_k u_k}(m, d) \triangleq \mathbb{E}[u_k(m)\, u_k^*(m - d)]$$

denotes the autocorrelation of $u_k(m)$, with $d \in \mathbb{Z}$. At this point, according to (2), it is useful to write the transmitted data block $u_k(m)$ as

$$u_k(m) = \sum_{\ell=0}^{M_{\mathrm{u}}-1} \sum_{r=-\infty}^{+\infty} \widetilde{s}_{k,\ell}(r)\, \rho_{k,\ell}(m - r\,P) \tag{29}$$

where $\widetilde{s}_{k,\ell}(n)$ is the $(\ell+1)$th element of $\widetilde{\mathbf{s}}_k(n)$, for $\ell \in \{0, 1, \ldots, M_{\mathrm{u}} - 1\}$, and $\rho_{k,\ell}(p) \triangleq M^{-1/2}\, e^{j\frac{2\pi}{M}(p - L_{\mathrm{cp}})\, i_{k,\ell}}\, \Pi_P(p)$. By virtue of (29), for $d = i_2 - i_1 \in \{-L_{\mathrm{g}}, \ldots, -1, 0, 1, \ldots, L_{\mathrm{g}}\}$, one obtains

$$R_{u_k u_k}(m, d) = \left[\frac{\sigma_s^2}{M} \sum_{\ell=0}^{M_{\mathrm{u}}-1} \left(e^{j\frac{2\pi}{M}\, d}\right)^{i_{k,\ell}}\right] \cdot \mathrm{rep}_P\left[\Pi_P(m)\, \Pi_P(m - d)\right] \tag{30}$$

where the factor in square brackets is a polynomial of degree $i_{k,M_{\mathrm{u}}-1}$ in the variable $e^{j\frac{2\pi}{M}\, d}$. Eq. (30) shows that $R_{u_k u_k}(m, d)$, as a function of m, can be periodic of period P and, thus, the random vector $\overline{\mathbf{u}}_k(n)$ can be wide-sense cyclostationary [42]: in such a case, the covariance matrix $\mathbf{R}_{\overline{\mathbf{u}}_k\overline{\mathbf{u}}_k}(m)$ is periodically time-varying (PTV) with period P. For instance, in the case of subband CAS, i.e., $i_{k,\ell} = \ell + \phi_k$,

for $\ell \in \{0,1,\ldots,M_{\rm u}-1\}$, one has

$$R_{u_k u_k}(m,d) = \left[\frac{\sigma_s^2}{M}\left(\frac{1-e^{j\frac{2\pi}{K_{\rm m}}d}}{1-e^{j\frac{2\pi}{M}d}}\right) e^{j\frac{2\pi}{M}d\,\phi_k}\right] \cdot \mathrm{rep}_P\left[\Pi_P(m)\,\Pi_P(m-d)\right]. \quad (31)$$

For an SC-IFDMA system employing interleaved CAS, instead, $i_{k,\ell} = \ell K_{\rm m} + \phi_k$ according to (1) and, hence, eq. (30) boils down to $R_{u_k u_k}(m,d) = \sigma_s^2\,\delta(d)\,\mathrm{rep}_P\left[\Pi_P(m)\right]$.

If $L_{\rm g} < M_{\rm u}$, it results that $\mathbf{R}_{\overline{\mathbf{u}}_k\overline{\mathbf{u}}_k}(m) \equiv \mathbf{R}_{\overline{\mathbf{u}}_k\overline{\mathbf{u}}_k} = \sigma_s^2\,\mathbf{I}_{L_{\rm g}+1}$ which, when substituted in (28), implies $\mathbf{R}_{\overline{\mathbf{r}}\overline{\mathbf{r}}}(m) \equiv \mathbf{R}_{\overline{\mathbf{r}}\overline{\mathbf{r}}}$, which can be written as

$$\mathbf{R}_{\overline{\mathbf{r}}\overline{\mathbf{r}}} = \sigma_s^2\,\mathbf{H}\,\mathbf{H}^H + \sigma_w^2\,\mathbf{I}_{Q(L_{\rm e}+1)} \quad (32)$$

where

$$\mathbf{H} \triangleq \left[\mathbf{\Sigma}_1\,\mathbf{H}_1, \mathbf{\Sigma}_2\,\mathbf{H}_2, \ldots, \mathbf{\Sigma}_K\,\mathbf{H}_K\right] \in \mathbb{C}^{Q(L_{\rm e}+1)\times K(L_{\rm g}+1)}.$$

Appendix B
Proof of Theorem 1

Let us rewrite (14), by exploiting the generalized sidelobe canceller (GSC) decomposition [34], as

$$\mathbf{f}_{\rm mmoe} = \mathbf{f}_{\rm mmoe}^{(0)} - \mathbf{\Pi}\,\mathbf{f}_{\rm mmoe}^{(a)}$$

where $\mathbf{f}_{\rm mmoe}^{(0)} \triangleq \mathbf{\Theta}_{L_{\rm eff}}\boldsymbol{\gamma} \in \mathbb{C}^{Q(L_{\rm e}+1)}$ satisfies the constraint $\mathbf{f}^H\mathbf{\Theta}_{L_{\rm eff}} = \boldsymbol{\gamma}^H$ by construction, the signal blocking matrix $\mathbf{\Pi} \in \mathbb{R}^{Q(L_{\rm e}+1)\times Q(L_{\rm e}-L_{\rm eff})}$ obeys $\mathbf{\Pi}^T\mathbf{\Theta}_{L_{\rm eff}} = \mathbf{O}_{Q(L_{\rm e}-L_{\rm eff})\times Q(L_{\rm eff}+1)}$, i.e., $\mathcal{R}(\mathbf{\Pi}) \equiv \mathcal{R}^{\perp}(\mathbf{\Theta}_{L_{\rm eff}})$, and $\mathbf{\Pi}^T\mathbf{\Pi} = \mathbf{I}_{Q(L_{\rm e}-L_{\rm eff})}$, whereas $\mathbf{f}_{\rm mmoe}^{(a)} \in \mathbb{C}^{Q(L_{\rm e}-L_{\rm eff})}$ is given by

$$\mathbf{f}_{\rm mmoe}^{(a)} = \left(\mathbf{\Pi}^T\,\mathbf{R}_{\overline{\mathbf{r}}\overline{\mathbf{r}}}\,\mathbf{\Pi}\right)^{-1}\mathbf{\Pi}^T\,\mathbf{R}_{\overline{\mathbf{r}}\overline{\mathbf{r}}}\,\mathbf{f}_{\rm mmoe}^{(0)} \quad (33)$$

Recalling that $\mathbf{f}_{\rm mmoe} = \mathbf{F}_{\rm mmoe}\boldsymbol{\gamma}$, with $\mathbf{F}_{\rm mmoe} \in \mathbb{C}^{Q(L_{\rm e}+1)\times Q(L_{\rm eff}+1)}$, one readily obtains (see, e.g., [43])

$$\mathbf{F}_{\rm mmoe} = \mathbf{\Theta}_{L_{\rm eff}} - \mathbf{\Pi}\left(\mathbf{\Pi}^T\,\mathbf{R}_{\overline{\mathbf{r}}\overline{\mathbf{r}}}\,\mathbf{\Pi}\right)^{-1}\mathbf{\Pi}^T\,\mathbf{R}_{\overline{\mathbf{r}}\overline{\mathbf{r}}}\,\mathbf{\Theta}_{L_{\rm eff}}. \quad (34)$$

Let $\mathbf{g}_k = \mathbf{H}_k^H\,\mathbf{\Sigma}_k^H\,\mathbf{f}_{\rm mmoe} = \mathbf{H}_k^H\,\mathbf{\Sigma}_k^H\,\mathbf{F}_{\rm mmoe}\,\boldsymbol{\gamma}$, substituting (32) (which holds since $L_{\rm g} < M_{\rm u}$) in (34), remembering that $\mathbf{\Pi}^T\mathbf{\Theta}_{L_{\rm eff}} = \mathbf{O}_{Q(L_{\rm e}-L_{\rm eff})\times Q(L_{\rm eff}+1)}$ and $\mathbf{\Pi}^T\mathbf{\Pi} = \mathbf{I}_{Q(L_{\rm e}-L_{\rm eff})}$, one has

$$\mathbf{H}^H\mathbf{F}_{\rm mmoe} = \mathbf{H}^H\left\{\mathbf{I}_{Q(L_{\rm e}+1)} - \sigma_s^2\,\mathbf{\Pi}\left[\sigma_s^2\,\mathbf{\Pi}^T\,\mathbf{H}\,\mathbf{H}^H\,\mathbf{\Pi} + \sigma_w^2\,\mathbf{I}_{Q(L_{\rm e}-L_{\rm eff})}\right]^{-1}\mathbf{\Pi}^T\,\mathbf{H}\,\mathbf{H}^H\right\}\mathbf{\Theta}_{L_{\rm eff}}. \quad (35)$$

Using the limit formula for the Moore-Penrose inverse [44], one obtains

$$\begin{aligned}\lim_{\sigma_s^2/\sigma_w^2\to+\infty}\mathbf{H}^H\mathbf{F}_{\rm mmoe} &= \mathbf{H}^H\left[\mathbf{I}_{Q(L_{\rm e}+1)} - \mathbf{\Pi}(\mathbf{H}^H\mathbf{\Pi})^{\dagger}\mathbf{H}^H\right]\mathbf{\Theta}_{L_{\rm eff}}\\ &= \left[\mathbf{I}_{K(L_{\rm g}+1)} - \mathbf{H}^H\mathbf{\Pi}(\mathbf{H}^H\mathbf{\Pi})^{\dagger}\right]\mathbf{H}^H\mathbf{\Theta}_{L_{\rm eff}}. \quad (36)\end{aligned}$$

For $k \in \{1,2,\ldots,K\}$, the kth block of

$$\mathbf{\Pi}^T\,\mathbf{H} = \left[\mathbf{\Pi}^T\,\mathbf{\Sigma}_1\,\mathbf{H}_1, \mathbf{\Pi}^T\,\mathbf{\Sigma}_2\,\mathbf{H}_2, \ldots, \mathbf{\Pi}^T\,\mathbf{\Sigma}_K\,\mathbf{H}_K\right]$$

can be expressed as

$$\begin{aligned}&\mathbf{\Pi}^T\,\mathbf{\Sigma}_k\,\mathbf{H}_k = [\mathbf{\Pi}^T\,\mathbf{\Theta}_{L_{\rm eff}}\,\mathbf{J}_{L_{\rm eff}}\cdots\mathbf{J}_1\,\overline{\mathbf{\Sigma}}_{k,0}\,\boldsymbol{\xi}_{k,0},\ldots,\\ &\mathbf{\Pi}^T\,\mathbf{\Theta}_{L_{\rm eff}}\,\mathbf{J}_{L_{\rm eff}}\,\overline{\mathbf{\Sigma}}_{k,L_{\rm eff}-1}\,\boldsymbol{\xi}_{k,L_{\rm eff}-1}, \mathbf{\Pi}^T\,\mathbf{\Theta}_{L_{\rm eff}}\,\overline{\mathbf{\Sigma}}_{k,L_{\rm eff}}\,\boldsymbol{\xi}_{k,L_{\rm eff}},\\ &\mathbf{\Pi}^T\,\mathbf{\Sigma}_k\,\mathbf{h}_{k,L_{\rm eff}+1}, \mathbf{\Pi}^T\,\mathbf{\Sigma}_k\,\mathbf{h}_{k,L_{\rm eff}+2},\ldots,\mathbf{\Pi}^T\,\mathbf{\Sigma}_k\,\mathbf{h}_{k,L_{\rm g}}]\\ &= \mathbf{\Pi}^T\,\mathbf{\Sigma}_k\,\mathbf{H}_{k,\rm wall}\,\mathbf{\Upsilon} \quad (37)\end{aligned}$$

with

$$\mathbf{H}_{k,\rm wall} \triangleq [\mathbf{h}_{k,L_{\rm eff}+1}, \mathbf{h}_{k,L_{\rm eff}+2},\ldots,\mathbf{h}_{k,L_{\rm g}}] \in \mathbb{C}^{Q(L_{\rm e}+1)\times(L_{\rm g}-L_{\rm eff})}$$
$$\mathbf{\Upsilon} \triangleq [\mathbf{O}_{(L_{\rm g}-L_{\rm eff})\times(L_{\rm eff}+1)}, \mathbf{I}_{L_{\rm g}-L_{\rm eff}}] \in \mathbb{C}^{(L_{\rm g}-L_{\rm eff})\times(L_{\rm g}+1)}$$

where we recall that $\mathbf{\Pi}^T\,\mathbf{\Theta}_{L_{\rm eff}} = \mathbf{O}_{Q(L_{\rm e}-L_{\rm eff})\times Q(L_{\rm eff}+1)}$. Thus, one gets $\mathbf{\Pi}^T\,\mathbf{H} = \mathbf{\Pi}^T\,\mathbf{H}_{\rm wall}\,(\mathbf{I}_K\otimes\mathbf{\Upsilon})$, where

$$\mathbf{H}_{\rm wall} \triangleq \left[\mathbf{\Sigma}_1\,\mathbf{H}_{1,\rm wall}, \mathbf{\Sigma}_2\,\mathbf{H}_{2,\rm wall},\ldots,\mathbf{\Sigma}_K\,\mathbf{H}_{K,\rm wall}\right].$$

Since $\mathrm{rank}(\mathbf{\Pi}^T\,\mathbf{H}_{\rm wall}) = K\,(L_{\rm g}-L_{\rm eff})$ by assumption, which requires that $Q\,(L_{\rm e}-L_{\rm eff}) \geq K\,(L_{\rm g}-L_{\rm eff})$, it follows [44] that $(\mathbf{\Pi}^T\,\mathbf{H})^{\dagger} = (\mathbf{I}_K\otimes\mathbf{\Upsilon})^{\dagger}\,(\mathbf{\Pi}^T\,\mathbf{H}_{\rm wall}\,\mathbf{\Xi})^{\dagger}$, where $\mathbf{\Xi} \triangleq (\mathbf{I}_K\otimes\mathbf{\Upsilon})\,(\mathbf{I}_K\otimes\mathbf{\Upsilon})^{\dagger} \in \mathbb{C}^{K(L_{\rm g}-L_{\rm eff})\times K(L_{\rm g}-L_{\rm eff})}$ is the orthogonal projector onto $\mathcal{R}(\mathbf{I}_K\otimes\mathbf{\Upsilon})$. It is seen that $(\mathbf{I}_K\otimes\mathbf{\Upsilon})^{\dagger} = (\mathbf{I}_K\otimes\mathbf{\Upsilon}^{\dagger})$, with $\mathbf{\Upsilon}^{\dagger} = \mathbf{\Upsilon}^T$, and, consequently, $\mathbf{\Xi} = \mathbf{I}_K\otimes(\mathbf{\Upsilon}\,\mathbf{\Upsilon}^T) = \mathbf{I}_{K(L_{\rm g}-L_{\rm eff})}$. Therefore, one has

$$\begin{aligned}(\mathbf{H}^H\,\mathbf{\Pi})^{\dagger} &= [(\mathbf{\Pi}^T\,\mathbf{H})^{\dagger}]^H = [(\mathbf{\Pi}^T\,\mathbf{H}_{\rm wall})^{\dagger}]^H\,[(\mathbf{I}_K\otimes\mathbf{\Upsilon})^{\dagger}]^H\\ &= (\mathbf{H}_{\rm wall}^H\,\mathbf{\Pi})^{\dagger}\,(\mathbf{I}_K\otimes\mathbf{\Upsilon}^H)^{\dagger} = (\mathbf{H}_{\rm wall}^H\,\mathbf{\Pi})^{\dagger}\\ &\cdot[\mathbf{I}_K\otimes(\mathbf{\Upsilon}^{\dagger})^H] = (\mathbf{H}_{\rm wall}^H\,\mathbf{\Pi})^{\dagger}\,(\mathbf{I}_K\otimes\mathbf{\Upsilon}) \quad (38)\end{aligned}$$

which can be substituted in (36), hence obtaining

$$\begin{aligned}&\lim_{\sigma_s^2/\sigma_w^2\to+\infty}\mathbf{H}^H\mathbf{F}_{\rm mmoe}\\ &= \left\{\mathbf{I}_{K(L_{\rm g}+1)} - [\mathbf{I}_K\otimes(\mathbf{\Upsilon}^H\mathbf{\Upsilon})]\right\}\mathbf{H}^H\mathbf{\Theta}_{L_{\rm eff}}\\ &= \left[\mathbf{I}_K\otimes(\mathbf{I}_{L_{\rm g}+1} - \mathbf{\Upsilon}^H\,\mathbf{\Upsilon})\right]\mathbf{H}^H\,\mathbf{\Theta}_{L_{\rm eff}}\\ &= \left\{\mathbf{I}_K\otimes\begin{bmatrix}\mathbf{I}_{L_{\rm eff}+1} & \mathbf{O}_{(L_{\rm eff}+1)\times(L_{\rm g}-L_{\rm eff})}\\ \mathbf{O}_{(L_{\rm g}-L_{\rm eff})\times(L_{\rm eff}+1)} & \mathbf{O}_{(L_{\rm g}-L_{\rm eff})\times(L_{\rm g}-L_{\rm eff})}\end{bmatrix}\right\}\\ &\cdot\mathbf{H}^H\,\mathbf{\Theta}_{L_{\rm eff}} \quad (39)\end{aligned}$$

where, since $\mathbf{H}_{\rm wall}^H\mathbf{\Pi}^T$ is full-row rank, it holds that $(\mathbf{H}_{\rm wall}^H\,\mathbf{\Pi}^T)\,(\mathbf{H}_{\rm wall}^H\,\mathbf{\Pi}^T)^{\dagger} = \mathbf{I}_{K(L_{\rm g}-L_{\rm eff})}$. By remembering the partitioned structure of $\mathbf{H}$, one obtains from (39) the K limit relations

$$\lim_{\sigma_s^2/\sigma_w^2\to+\infty}\mathbf{g}_k = \begin{bmatrix}\mathbf{H}_{k,\rm win}^H\,\mathbf{\Sigma}_k^H\,\mathbf{\Theta}_{L_{\rm eff}}\boldsymbol{\gamma}\\ \mathbf{0}_{(L_{\rm g}-L_{\rm eff})}\end{bmatrix} \quad (40)$$

for $k \in \{1,2,\ldots,K\}$, where

$$\mathbf{H}_{k,\rm win} \triangleq [\mathbf{h}_{k,0}, \mathbf{h}_{k,1},\ldots,\mathbf{h}_{k,L_{\rm eff}}] \in \mathbb{C}^{Q(L_{\rm e}+1)\times(L_{\rm eff}+1)}.$$

Appendix C
Expression of the matrix $\mathbf{Z}(n)$

Using (16), one obtains

$$\mathbf{Z}(n) = \sum_{k=1}^{K} e^{j\frac{2\pi}{M}\epsilon_k(nP+L_{\rm cp})}\,\mathbf{\Omega}_k\,\overline{\mathbf{U}}_{k,\rm win}(n)\,\mathbf{G}_{k,\rm win}^* + \mathbf{V}(n)$$

where

$$\begin{aligned}\boldsymbol{\Omega}_k &\triangleq \mathrm{diag}[1, e^{j\frac{2\pi}{M}\epsilon_k}, \ldots, e^{j\frac{2\pi}{M}\epsilon_k(M-1)}] \in \mathbb{C}^{M\times M}\\ \overline{\mathbf{U}}_{k,\mathrm{win}}(n) &\triangleq [\overline{\mathbf{u}}_{k,\mathrm{win}}(nP+L_{\mathrm{cp}}), \ldots, \overline{\mathbf{u}}_{k,\mathrm{win}}(nP+P-1)]^T\\ \mathbf{V}(n) &\triangleq [\mathbf{v}(nP+L_{\mathrm{cp}}), \ldots, \mathbf{v}(nP+P-1)]^T. \end{aligned} \quad (41)$$

By observing that

$$\overline{\mathbf{u}}_{k,\mathrm{win}}(m) = [u_k(m), u_k(m-1), \ldots, u_k(m-L_{\mathrm{cp}})]^T \in \mathbb{C}^{L_{\mathrm{cp}}+1}$$

taking into account (2), and remembering that $u_k(nP+p) = u_{k,p}(n)$ for $p \in \{0,1,\ldots,P-1\}$, it can be readily verified that $\overline{\mathbf{U}}_{k,\mathrm{win}}(n) = \overline{\boldsymbol{\mathcal{U}}}_{k,\mathrm{win}}(n)\,\overline{\mathbf{C}}$, where the circulant matrix $\overline{\boldsymbol{\mathcal{U}}}_{k,\mathrm{win}}(n) \in \mathbb{C}^{M\times M}$ has $\mathbf{W}_k\,\widetilde{\mathbf{s}}_k(n)$ as first column and

$$\overline{\mathbf{C}} \triangleq [\mathbf{I}_{L_{\mathrm{cp}}+1}, \mathbf{O}_{(L_{\mathrm{cp}}+1)\times(M-L_{\mathrm{cp}}-1)}]^T \in \mathbb{R}^{M\times(L_{\mathrm{cp}}+1)}.$$

For $i \in \{0,1,\ldots,Q(L_{\mathrm{cp}}+1)-1\}$, let $\mathbf{z}_i(n) \in \mathbb{C}^M$ and $\mathbf{v}_i(n) \in \mathbb{C}^M$ denote the ith column of $\mathbf{Z}(n)$ and $\mathbf{V}(n)$, respectively, by exploiting the circulant structure of $\overline{\boldsymbol{\mathcal{U}}}_{k,\mathrm{win}}(n)$, it can be shown that

$$\mathbf{z}_i(n) = \sum_{k=1}^{K} e^{j\frac{2\pi}{M}\epsilon_k(nP+L_{\mathrm{cp}})}\,\boldsymbol{\Omega}_k\,\mathbf{G}_{k,i}\,\mathbf{W}_k\,\widetilde{\mathbf{s}}_k(n) + \mathbf{v}_i(n) \quad (42)$$

where $\mathbf{G}_{k,i} \in \mathbb{C}^{M\times M}$ is the circulant matrix having

$$[\{\mathbf{G}_{k,\mathrm{win}}\}_{0,i}, \{\mathbf{G}_{k,\mathrm{win}}\}_{1,i} \ldots, \{\mathbf{G}_{k,\mathrm{win}}\}_{L_{\mathrm{cp}},i}, 0, \ldots, 0]^H$$

as first column. Taking into account (1), it can be verified that $\mathbf{W}_k = \boldsymbol{\Delta}_k\left(\mathbf{1}_{K_{\mathrm{m}}} \otimes \mathbf{W}_{\mathrm{dft}}^{-1}\right)$, where $\boldsymbol{\Delta}_k \triangleq K_{\mathrm{m}}^{-1/2}\,\mathrm{diag}[1, e^{j\frac{2\pi}{M}\phi_k}, \ldots, e^{j\frac{2\pi}{M}\phi_k(M-1)}] \in \mathbb{C}^{M\times M}$. Thus, remembering that $\widetilde{\mathbf{s}}_k(n) = \mathbf{W}_{\mathrm{dft}}\,\mathbf{s}_k(n)$, one has $\mathbf{W}_k\,\widetilde{\mathbf{s}}_k(n) = \boldsymbol{\Delta}_k\,[\mathbf{1}_{K_{\mathrm{m}}} \otimes \mathbf{s}_k(n)]$, which represents a matrix formulation of the well-known result [7] that the interleaved CAS of an SC-IFDMA symbol can be implemented in the time domain by first repeating K_{m} times the block $\mathbf{s}_k(n)$ and, then, multiplying the result by complex exponentials to perform frequency shifts. By exploiting the circulant structure of $\mathbf{G}_{k,i}$, it can be shown that $\mathbf{G}_{k,i}\,\boldsymbol{\Delta}_k = \boldsymbol{\Delta}_k\,\boldsymbol{\mathcal{G}}_{k,i}$, where $\boldsymbol{\mathcal{G}}_{k,i} \in \mathbb{C}^{M\times M}$ is the circulant matrix having $[\{\mathbf{G}_{k,\mathrm{win}}\}_{0,i}, \{\mathbf{G}_{k,\mathrm{win}}\}_{1,i}\,e^{j\frac{2\pi}{M}\phi_k}, \ldots, \{\mathbf{G}_{k,\mathrm{win}}\}_{L_{\mathrm{cp}},i}\,e^{j\frac{2\pi}{M}\phi_k L_{\mathrm{cp}}}, 0, \ldots, 0]^H$ as first column, which can be partitioned as

$$\boldsymbol{\mathcal{G}}_{k,i} = \begin{bmatrix} \boldsymbol{\mathcal{G}}_{k,i}^{(0)} & \boldsymbol{\mathcal{G}}_{k,i}^{(1)} & \ldots & \boldsymbol{\mathcal{G}}_{k,i}^{(K_{\mathrm{m}}-2)} & \boldsymbol{\mathcal{G}}_{k,i}^{(K_{\mathrm{m}}-1)} \\ \boldsymbol{\mathcal{G}}_{k,i}^{(K_{\mathrm{m}}-1)} & \boldsymbol{\mathcal{G}}_{k,i}^{(0)} & \ldots & \boldsymbol{\mathcal{G}}_{k,i}^{(K_{\mathrm{m}}-3)} & \boldsymbol{\mathcal{G}}_{k,i}^{(K_{\mathrm{m}}-2)} \\ \vdots & \vdots & \vdots & \vdots & \vdots \\ \boldsymbol{\mathcal{G}}_{k,i}^{(1)} & \boldsymbol{\mathcal{G}}_{k,i}^{(2)} & \ldots & \boldsymbol{\mathcal{G}}_{k,i}^{(K_{\mathrm{m}}-1)} & \boldsymbol{\mathcal{G}}_{k,i}^{(0)} \end{bmatrix} \quad (43)$$

with $\boldsymbol{\mathcal{G}}_{k,i}^{(r)} \in \mathbb{C}^{M_{\mathrm{u}}\times M_{\mathrm{u}}}$, for $r \in \{0,1,\ldots,K_{\mathrm{m}}-1\}$. As a consequence of the aforementioned rearrangements, by partitioning

$$\begin{aligned}\boldsymbol{\Omega}_k &= \mathrm{diag}[\boldsymbol{\Omega}_k^{(0)}, \boldsymbol{\Omega}_k^{(1)}, \ldots, \boldsymbol{\Omega}_k^{(K_{\mathrm{m}}-1)}]\\ \boldsymbol{\Delta}_k &= \mathrm{diag}[\boldsymbol{\Delta}_k^{(0)}, \boldsymbol{\Delta}_k^{(1)}, \ldots, \boldsymbol{\Delta}_k^{(K_{\mathrm{m}}-1)}] \end{aligned} \quad (44)$$

with $\boldsymbol{\Omega}_k^{(r)} \in \mathbb{C}^{M_{\mathrm{u}}\times M_{\mathrm{u}}}$ and $\boldsymbol{\Delta}_k^{(r)} \in \mathbb{C}^{M_{\mathrm{u}}\times M_{\mathrm{u}}}$, and defining

$$\begin{aligned}\boldsymbol{\Psi}_k^{(r)} \triangleq \boldsymbol{\Omega}_k^{(r)}\,\boldsymbol{\Delta}_k^{(r)} = K_{\mathrm{m}}^{-1/2}\mathrm{diag}\Big[&e^{j\frac{2\pi}{M}rM_{\mathrm{u}}(\epsilon_k+\phi_k)}, \ldots,\\ &e^{j\frac{2\pi}{M}(rM_{\mathrm{u}}+M_{\mathrm{u}}-1)(\epsilon_k+\phi_k)}\Big] \in \mathbb{C}^{M_{\mathrm{u}}\times M_{\mathrm{u}}}\end{aligned} \quad (45)$$

for $k \in \{1,2,\ldots,K\}$ and $r \in \{0,1,\ldots,K_{\mathrm{m}}-1\}$, eq. (42) can be rewritten as

$$\mathbf{z}_i(n) = \sum_{k=1}^{K} e^{j\frac{2\pi}{M}\epsilon_k(nP+L_{\mathrm{cp}})}\,\boldsymbol{\Psi}_k\,\widetilde{\boldsymbol{\mathcal{G}}}_{k,i}\,\mathbf{s}_k(n) + \mathbf{v}_i(n) \quad (46)$$

where $\boldsymbol{\Psi}_k \triangleq [\boldsymbol{\Psi}_k^{(0)}, \boldsymbol{\Psi}_k^{(1)}, \ldots, \boldsymbol{\Psi}_k^{(K_{\mathrm{m}}-1)}]^T \in \mathbb{C}^{M\times M_{\mathrm{u}}}$ and, provided that $L_{\mathrm{cp}} \leq M_{\mathrm{u}}$, the circulant matrix $\widetilde{\boldsymbol{\mathcal{G}}}_{k,i} \triangleq \sum_{r=0}^{K_{\mathrm{m}}-1}\boldsymbol{\mathcal{G}}_{k,i}^{(r)} \in \mathbb{C}^{M_{\mathrm{u}}\times M_{\mathrm{u}}}$ has $[\{\mathbf{G}_{k,\mathrm{win}}\}_{0,i}, \{\mathbf{G}_{k,\mathrm{win}}\}_{1,i}\,e^{j\frac{2\pi}{M}\phi_k}, \ldots, \{\mathbf{G}_{k,\mathrm{win}}\}_{L_{\mathrm{cp}},i}\,e^{j\frac{2\pi}{M}\phi_k L_{\mathrm{cp}}}, 0, \ldots, 0]^H$ as first column. Finally, by defining

$$\begin{aligned}\boldsymbol{\Psi} &\triangleq [\boldsymbol{\Psi}_1, \boldsymbol{\Psi}_2, \ldots, \boldsymbol{\Psi}_K] \in \mathbb{C}^{M\times KM_{\mathrm{u}}}\\ \mathbf{a}_i(n) &\triangleq [\{e^{j\frac{2\pi}{M}\epsilon_1(nP+L_{\mathrm{cp}})}\,\widetilde{\boldsymbol{\mathcal{G}}}_{1,i}\,\mathbf{s}_1(n)\}^T, \ldots,\\ &\quad \{e^{j\frac{2\pi}{M}\epsilon_K(nP+L_{\mathrm{cp}})}\,\widetilde{\boldsymbol{\mathcal{G}}}_{K,i}\,\mathbf{s}_K(n)\}^T]^T \in \mathbb{C}^{KM_{\mathrm{u}}}\end{aligned}$$

eq. (46) can be compactly expressed as $\mathbf{z}_i(n) = \boldsymbol{\Psi}\,\mathbf{a}_i(n) + \mathbf{v}_i(n)$, from which (17) easily follows.

APPENDIX D
FULL-COLUMN RANK PROPERTY OF THE MATRIX $\boldsymbol{\Psi}$

The matrix $\boldsymbol{\Psi}$ is full-column rank, i.e., $\mathrm{rank}(\boldsymbol{\Psi}) = K\,M_{\mathrm{u}}$, if and only if the null space of $\boldsymbol{\Psi}$ is trivial, i.e., $\mathcal{N}(\boldsymbol{\Psi}) \equiv \{\mathbf{0}_{KM_{\mathrm{u}}}\}$, which necessarily requires that $K\,M_{\mathrm{u}} \leq M$. A vector $\boldsymbol{\beta} \triangleq [\boldsymbol{\beta}_1^T, \boldsymbol{\beta}_2^T, \ldots, \boldsymbol{\beta}_K^T]^T \in \mathbb{C}^{KM_{\mathrm{u}}}$, with $\boldsymbol{\beta}_k = [\beta_{k,0}, \beta_{k,1}, \ldots, \beta_{k,M_{\mathrm{user}}-1}]^T \in \mathbb{C}^{M_{\mathrm{u}}}$ for $k \in \{1,2,\ldots,K\}$, belonging to $\mathcal{N}(\boldsymbol{\Psi})$ obeys $\boldsymbol{\Psi}\,\boldsymbol{\beta} = \mathbf{0}_M$. By exploiting the block structure of $\boldsymbol{\Psi}$ and $\{\boldsymbol{\Psi}_k\}_{k=1}^K$, one has

$$\boldsymbol{\Psi}\,\boldsymbol{\beta} = \mathbf{0}_M \iff \sum_{k=1}^{K}\boldsymbol{\Psi}_k\,\boldsymbol{\beta}_k = \mathbf{0}_M \iff \boldsymbol{\mathcal{V}}\,\widetilde{\boldsymbol{\beta}} = \mathbf{0}_M \quad (47)$$

where the ℓth diagonal block of the matrix $\boldsymbol{\mathcal{V}} \triangleq \mathrm{diag}[\boldsymbol{\mathcal{V}}_0, \boldsymbol{\mathcal{V}}_1, \ldots, \boldsymbol{\mathcal{V}}_{M_{\mathrm{u}}-1}] \in \mathbb{C}^{M\times(KM_{\mathrm{u}})}$ is given by $\boldsymbol{\mathcal{V}}_\ell = \widetilde{\boldsymbol{\mathcal{V}}}\,\mathrm{diag}[e^{j\frac{2\pi}{M}(\epsilon_1+\phi_1)\ell}, e^{j\frac{2\pi}{M}(\epsilon_2+\phi_2)\ell}, \ldots, e^{j\frac{2\pi}{M}(\epsilon_K+\phi_K)\ell}]$ for $\ell \in \{0,1,\ldots,M_{\mathrm{u}}-1\}$, with $\widetilde{\boldsymbol{\mathcal{V}}} \in \mathbb{C}^{K_{\mathrm{m}}\times K}$ being the Vandermonde matrix associated with the vector $[e^{j\frac{2\pi}{K_{\mathrm{m}}}(\epsilon_1+\phi_1)}, e^{j\frac{2\pi}{K_{\mathrm{m}}}(\epsilon_2+\phi_2)}, \ldots, e^{j\frac{2\pi}{K_{\mathrm{m}}}(\epsilon_K+\phi_K)}]^T$, and, finally, $\widetilde{\boldsymbol{\beta}} \triangleq [\beta_{1,0}, \ldots, \beta_{K,0}, \beta_{1,1}, \ldots, \beta_{K,1}, \ldots, \beta_{1,M_{\mathrm{u}}-1}, \ldots, \beta_{K,M_{\mathrm{u}}-1}]^T \in \mathbb{C}^{KM_{\mathrm{u}}}$. Since $K_{\mathrm{m}} \geq K$, matrix $\widetilde{\boldsymbol{\mathcal{V}}}$ is full-column rank, provided that $e^{j\frac{2\pi}{K_{\mathrm{m}}}(\epsilon_1+\phi_1)} \neq e^{j\frac{2\pi}{K_{\mathrm{m}}}(\epsilon_2+\phi_2)} \neq \cdots \neq e^{j\frac{2\pi}{K_{\mathrm{m}}}(\epsilon_K+\phi_K)}$. In such a case, each block $\boldsymbol{\mathcal{V}}_\ell$ is full-column rank in its turn, i.e., $\mathrm{rank}(\boldsymbol{\mathcal{V}}_\ell) = K$, thus implying that $\mathrm{rank}(\boldsymbol{\mathcal{V}}) = \sum_{\ell=0}^{M_{\mathrm{u}}-1}\mathrm{rank}(\boldsymbol{\mathcal{V}}_\ell) = K\,M_{\mathrm{u}}$. Hence, matrix $\boldsymbol{\mathcal{V}}$ is full-column rank and, consequently, the unique solution of $\boldsymbol{\mathcal{V}}\,\widetilde{\boldsymbol{\beta}} = \mathbf{0}_M$ is $\widetilde{\boldsymbol{\beta}} = \mathbf{0}_{KM_{\mathrm{u}}}$, which leads to $\boldsymbol{\beta} = \mathbf{0}_{KM_{\mathrm{u}}}$.

APPENDIX E
EVALUATION OF THE COVARIANCE MATRIX OF $\mathbf{N}_k(n)$

Remembering that $\boldsymbol{\Psi}^\dagger = (\boldsymbol{\Psi}^H\boldsymbol{\Psi})^{-1}\boldsymbol{\Psi}^H$, let us partition $(\boldsymbol{\Psi}^H\boldsymbol{\Psi})^{-1}$ as

$$(\boldsymbol{\Psi}^H\boldsymbol{\Psi})^{-1} = \begin{bmatrix} \widetilde{\boldsymbol{\Psi}}_{1,1} & \widetilde{\boldsymbol{\Psi}}_{1,2} & \ldots & \widetilde{\boldsymbol{\Psi}}_{1,K} \\ \widetilde{\boldsymbol{\Psi}}_{2,1} & \widetilde{\boldsymbol{\Psi}}_{2,2} & \ldots & \widetilde{\boldsymbol{\Psi}}_{2,K} \\ \vdots & \vdots & \ddots & \vdots \\ \widetilde{\boldsymbol{\Psi}}_{K,1} & \widetilde{\boldsymbol{\Psi}}_{K,2} & \ldots & \widetilde{\boldsymbol{\Psi}}_{K,K} \end{bmatrix} \quad (48)$$

with $\widetilde{\mathbf{\Psi}}_{k,\ell} \in \mathbb{C}^{M_{\mathrm{u}} \times M_{\mathrm{u}}}$, for $k, \ell \in \{1, 2, \ldots, K\}$. It is shown in [7, App. A] that

$$\begin{aligned} \widetilde{\mathbf{\Psi}}_{k,\ell} &= \mu_{k,\ell}\, \widetilde{\mathbf{\Psi}}(\vartheta_\ell - \vartheta_k) \\ \mu_{k,\ell} &\triangleq \left\{ (\mathbf{\Psi}^H \mathbf{\Psi})^{-1} \right\}_{(k-1)M_{\mathrm{u}}+1,(\ell-1)M_{\mathrm{u}}+1} \\ \widetilde{\mathbf{\Psi}}(x) &\triangleq \mathrm{diag}[1, e^{j\frac{2\pi}{M}x}, \ldots, e^{j\frac{2\pi}{M}(M_{\mathrm{u}}-1)x}] \in \mathbb{C}^{M_{\mathrm{u}} \times M_{\mathrm{u}}} \\ \vartheta_k &\triangleq \epsilon_k + \phi_k \end{aligned} \tag{49}$$

for $k \in \{1, 2, \ldots, K\}$. By observing that

$$\begin{aligned} \mathbf{\Omega}_k^{(r)} &= e^{j\frac{2\pi}{K_{\mathrm{m}}}\epsilon_k r}\, \widetilde{\mathbf{\Psi}}(\epsilon_k) \\ \mathbf{\Delta}_k^{(r)} &= K_{\mathrm{m}}^{-1/2}\, e^{j\frac{2\pi}{K_{\mathrm{m}}}\phi_k r}\, \widetilde{\Psi}(\phi_k) \end{aligned} \tag{50}$$

for $r \in \{0, 1, \ldots, K_{\mathrm{m}} - 1\}$, one has

$$\mathbf{R}_k\, \mathbf{\Psi}^\dagger = \mu_k\, \widetilde{\mathbf{\Psi}}^*(\vartheta_k) \left[\mathbf{I}_{M_{\mathrm{u}}}, e^{-j\frac{2\pi}{K_{\mathrm{m}}}\vartheta_k}\, \mathbf{I}_{M_{\mathrm{u}}}, \ldots, e^{-j\frac{2\pi}{K_{\mathrm{m}}}\vartheta_k (K_{\mathrm{m}}-1)}\, \mathbf{I}_{M_{\mathrm{u}}} \right]$$

where $\mu_k \triangleq K_{\mathrm{m}}^{-1/2} \sum_{\ell=1}^{K} \mu_{k,\ell}$. By introducing the partition $\overline{\mathbf{W}}(n) = [\overline{\mathbf{W}}_0^T(n), \overline{\mathbf{W}}_1^T(n), \ldots, \overline{\mathbf{W}}_{K_{\mathrm{m}}-1}^T(n)]^T$, with $\overline{\mathbf{W}}_r(n) \in \mathbb{C}^{M_{\mathrm{u}} \times Q(L_{\mathrm{e}}+1)}$, for $r \in \{0, 1, \ldots, K_{\mathrm{m}}-1\}$, we obtain

$$\mathbf{N}_k(n) = \mu_k\, \widetilde{\mathbf{\Psi}}^*(\vartheta_k) \sum_{r=0}^{K_{\mathrm{m}}-1} e^{-j\frac{2\pi}{K_{\mathrm{m}}}\vartheta_k r}\, \overline{\mathbf{W}}_r(n) \tag{51}$$

from which it readily follows that

$$\mathbf{R}_{\mathbf{N}_k \mathbf{N}_k} = M_{\mathrm{u}}\, \sigma_w^2\, |\mu_k|^2\, \mathbf{I}_{Q(L_{\mathrm{e}}+1)}\ .$$

REFERENCES

[1] H. Sari and G. Karam, "Orthogonal frequency-division multiple access and its application to CATV networks," *Eur. Trans. Commun.*, vol. 45, pp. 507–516, Nov.-Dic. 1998.

[2] "Interaction Channel for Digital Terrestrial Television (RCT) Incorporating Multiple Access OFDM," *ETSI DVB RCT*, Mar. 2001.

[3] K. Lu, Y. Qian, and H.-H. Chen, "Wireless broadband access: WiMAX and beyond – A secure and service-oriented network control framework for WiMAX networks," *IEEE Commun. Mag.*, vol. 45, pp. 124–130, May 2007.

[4] R. van Nee and R. Prasad, *OFDM for Wireless Multimedia Communications*. Artech House, 2000.

[5] T. Frank, A. Klein, and E. Costa, "IFDMA: a scheme combining the advantages of OFDMA and CDMA," *IEEE Wireless Commun.*, pp. 9–17, June 2007.

[6] M. Morelli, C.-C.J. Kuo, and M.-O. Pun, "Synchronization techniques for orthogonal frequency division multiple access (OFDMA): a tutorial review," *Proc. IEEE*, vol. 95, pp. 1394–1427, July 2007.

[7] Y. Zhu and K.B. Letaief, "CFO estimation and compensation in SC-IFDMA systems," *IEEE Trans. Wireless Commun.*, vol. 9, pp. 3200–3212, Oct. 2010.

[8] Z. Cao, U. Tureli, and Y.-D. Yao, "Deterministic multiuser carrier-frequency offset estimation for interleaved OFDMA uplink," *IEEE Trans. Commun.*, vol. 52, pp. 1585 – 1594, Sep. 2004.

[9] Z. Cao, U. Tureli, and Y.-D. Yao, "Low-complexity orthogonal spectral signal reconstruction for generalized OFDMA uplink with frequency synchronization errors," *IEEE Trans. Veh. Technol.*, vol. 56, pp. 1143 – 1154, May 2007.

[10] J. Lee, S. Lee, K.-J. Bang, S. Cha, and D. Hong, "Carrier frequency offset estimation using ESPRIT for interleaved OFDMA uplink systems," *IEEE Trans. Veh. Technol.*, vol. 56, pp. 3227 – 3231, Sep. 2007.

[11] P.J.W. Melsa, R.C. Younce, and C.E. Rohrs, "Impulse response shortening for discrete multitone transceivers," *IEEE Trans. Commun.*, vol. 44, pp. 1662–1672, Dec. 1996.

[12] C. Yin and G. Yue, "Optimal impulse response shortening for discrete multitone transceivers," *Electronics Letters*, vol. 34, pp. 35–36, Jan. 1998.

[13] A. Tkacenko and P.P. Vaidyanathan, "A low-complexity eigenfilter design method for channel shortening equalizers for DMT systems," *IEEE Trans. Commun.*, vol. 51, pp. 1069–1072, July 2003.

[14] N. Al-Dhahir and J.M. Cioffi, "Optimum finite-length equalization for multicarrier transceivers," *IEEE Trans. Commun.*, vol. 44, pp. 56–64, Jan. 1996.

[15] D. Daly, C. Heneghan, and A.D. Fagan, "Minimum mean-squared error impulse response shortening for discrete multitone transceivers", *IEEE Trans. Signal Process.*, vol. 52, pp. 301-306, Jan. 2004.

[16] G. Arslan, B. Evans, and S. Kiaei, "Equalization for discrete multitone transceivers to maximize bit rate", *IEEE Trans. Signal Process.*, vol. 49, pp. 3123-3135, Dec. 2001.

[17] S. Celebi, "Interblock interference (IBI) minimizing time-domain equalizer (TEQ) for OFDM", *IEEE Signal Process. Lett.*, vol. 10, pp. 232–234, Aug. 2003.

[18] R.K. Martin, J. Balakrishnan, W.A. Sethares, and C.R. Johnson, "A blind adaptive TEQ for multicarrier systems", *IEEE Signal Process. Lett.*, vol. 9, pp. 341–343, Nov. 2002.

[19] J. Balakrishnan, R.K. Martin, and C.R. Johnson, "Blind adaptive channel shortening by sum-squared auto-correlation minimization (SAM)", *IEEE Trans. Signal Process.*, vol. 51, pp. 3086–3093, Dec. 2003.

[20] R.K. Martin, "Joint blind adaptive carrier frequency offset estimation and channel shortening", *IEEE Trans. Signal Process.*, vol. 54, pp. 4194-4203, Nov. 2006.

[21] R.K. Martin, "Fast-converging blind adaptive channel-shortening and frequency-domain equalization", *IEEE Trans. Signal Process.*, vol. 55, pp. 102-110, Jan. 2007.

[22] T. Miyajima and Z. Ding, "Second-order statistical approaches to channel shortening in multicarrier systems", *IEEE Trans. Signal Process.*, vol. 52, pp. 3253–3264, Nov. 2004.

[23] D. Darsena and F. Verde, "A blind direct channel-shortening approach for multicarrier systems", in *Proc. of VIII IEEE Workshop on Signal Process. Advances in Wireless Commun. (SPAWC)*, Helsinki (Finland), June 2007, pp. 1–5.

[24] D. Darsena and F. Verde, "Minimum-mean-output-energy blind adaptive channel shortening for multicarrier SIMO transceivers," *IEEE Trans. Signal Process.*, vol. 55, pp. 5755–5771, Jan. 2007.

[25] N. Al-Dhahir, "FIR channel-shortening equalizers for MIMO ISI channels," *IEEE Trans. Commun.*, vol. 49, pp. 213–218, Feb. 2001.

[26] C. Toker, S. Lambotharan, J.A. Chambers, and B. Baykal, "Joint spatial and temporal channel-shortening techniques for frequency selective fading MIMO channels," *IEE Proc. Commun.*, vol. 152, pp. 89 – 94, Feb. 2005.

[27] R.K. Martin, G. Ysebaert, and K. Vanbleu, "Bit error rate minimizing channel shortening equalizers for cyclic prefixed systems", *IEEE Trans. Signal Process.*, vol. 55, pp. 2605-2616, June 2007.

[28] R.K. Martin, J.M. Walsh, and C.R. Johnson, "Low-complexity MIMO blind adaptive channel shortening", *IEEE Trans. Signal Process.*, vol. 53, pp. 1324-1334, Apr. 2005.

[29] G. Altin and R.K. Martin, "Adaptive MIMO channel shortening with post-FEQ diversity combining," in *Proc. IEEE Asilomar Conf. Signals, Systems, Comp.*, Pacific Grove, CA, USA, Nov. 2008, pp. 2183–2187.

[30] D. Darsena, G. Gelli, L. Paura, and F. Verde, "Blind channel shortening for space-time-frequency block coded MIMO-OFDM systems," *IEEE Trans. Wireless Commun.*, vol. 11, pp. 1022 – 1033, Mar. 2012.

[31] T. Miyajima and Z. Ding, "Subcarrier nulling algorithms for channel shortening in uplink OFDMA systems", *IEEE Trans. Signal Process.*, vol. 60, pp. 2374–2385, May 2012.

[32] B. Razavi, *RF Microelectronics*. Englewood Cliffs, NJ: Prentice-Hall, 1998.

[33] D. Tandur and M. Moonen, "Joint adaptive compensation of transmitter and receiver IQ imbalance under carrier frequency offset in OFDM-based systems", *IEEE Trans. Signal Process.*, vol. 55, pp. 5246–5252, Nov. 2007.

[34] L. J. Griffiths and C. W. Jim, "An alternative approach to linearly constrained adaptive beamforming," *IEEE Trans. Antennas Propag.*, vol. AP-30, pp. 27–34, Jan. 1982

[35] D. Darsena, G. Gelli, L. Paura, and F. Verde, "Blind periodically time-varying MMOE channel shortening for OFDM systems," in *Proc. IEEE International Conf. Acoustics, Speech and Signal Proc.*, Prague, Czech Republic, May 2011, pp. 3576– 3579.

[36] L. Franks, "Polyperiodic linear filtering," in *Cyclostationarity in Commun. and Signal Processing*, edited by W.A. Gardner, IEEE Press, 1994.

[37] F. Qian and B.D. Van Veen, "Quadratically constrained adaptive beamforming for coherent signals and interference," *IEEE Trans. Signal Process.*, vol. 43, pp. 1890 – 1900, Aug. 1995.

[38] M. Tanda and T. Fusco, "ML-based symbol timing and frequency offset estimation for OFDM systems with noncircular transmissions," *IEEE Trans. Signal Process.*, vol. 54, pp. 3527-3541, Sept. 2006.
[39] U. Mengali and A. N. D'Andrea, *Synchronization Techniques for Digital Receivers*. New York: Plenum, 1997.
[40] A.S. Cacciapuoti, G. Gelli, L. Paura, and F. Verde, "Finite-sample performance analysis of widely linear multiuser receivers for DS-CDMA systems," *IEEE Trans. Signal Process.*, vol. 56, no. 4, pp. 1572-1588, Apr. 2008.
[41] M.-O. Pun, M. Morelli, and C.-C. J. Kuo, "Maximum-likelihood synchronization and channel estimation for OFDMA uplink transmissions," *IEEE Trans. Commun.*, vol. 54, no. 4, pp. 726-736, Apr. 2006.
[42] W. A. Gardner, A. Napolitano, and L. Paura, "Cyclostationarity: Half a century of research," in *Signal Processing* (Elsevier), vol. 86, pp. 639 – 697, Apr. 2006.
[43] G. Gelli and F. Verde, "Two-stage interference-resistant adaptive periodically time-varying CMA blind equalization," *IEEE Trans. Signal Process.*, vol. 50, pp. 662–672, Mar. 2002.
[44] A. Ben-Israel and T. N. E. Greville, *Generalized Inverses*. New York: Springer-Verlag, 2002.

Donatella Darsena (M'06) received the Dr. Eng. degree *summa cum laude* in telecommunications engineering in 2001, and the Ph.D. degree in electronic and telecommunications engineering in 2005, both from the University of Napoli Federico II, Italy.

From 2001 to 2002, she was an engineer in the Telecommunications, Peripherals and Automotive Group, STMicroelectronics, Milano, Italy. Since 2005, she has been an Assistant Professor with the Department for Technologies, University of Napoli Parthenope, Italy. She has also held teaching positions at the University of Napoli Federico II, Italy. Her research activities lie in the area of statistical signal processing, digital communications, and communication systems. In particular, her current interests are focused on equalization, channel identification, narrowband-interference suppression for multicarrier systems, space-time processing for cooperative communications systems and cognitive communications systems, and software-defined networks.

Giacinto Gelli was born in Napoli, Italy, on July 29, 1964. He received the Dr. Eng. degree *summa cum laude* in electronic engineering in 1990, and the Ph.D. degree in computer science and electronic engineering in 1994, both from the University of Napoli Federico II.

From 1994 to 1998, he was an Assistant Professor with the Department of Information Engineering, Second University of Napoli. Since 1998 he has been with the Department of Biomedical, Electronic and Telecommunication Engineering, University of Napoli Federico II, first as an Associate Professor, and since November 2006 as a Full Professor of Telecommunications. He also held teaching positions at the University Parthenope of Napoli. His research interests are in the fields of statistical signal processing, array processing, image processing, and wireless communications, with current emphasis on code-division multiple-access systems and multicarrier modulation.

Luigi Paura (M'11) was born in Napoli, Italy, on February 20, 1950. He received the Dr. Eng. degree *summa cum laude* in electronic engineering in 1974 from the University of Napoli Federico II.

From 1979 to 1984 he was with the Department of Biomedical, Electronic and Telecommunication Engineering, University of Napoli, Italy, first as an Assistant Professor and then as an Associate Professor. Since 1994, he has been a Full Professor of Telecommunications: first, with the Department of Mathematics, University of Lecce, Italy; then, with the Department of Information Engineering, Second University of Napoli; and, finally, from 1998 he has been with the Department of Biomedical, Electronic and Telecommunication Engineering, University of Napoli Federico II. He also held teaching positions at the University of Salerno, at the University of Sannio, and at the University Parthenope of Napoli, In 1985-86 and 1991 he was a Visiting Researcher at the Signal and Image Processing Laboratory, University of California, Davis. At the present time, his research activities are mainly concerned with statistical signal processing, digital communication systems, and medium access control in wireless networks.

Francesco Verde (M'10) was born in Santa Maria Capua Vetere, Italy, on June 12, 1974. He received the Dr. Eng. degree *summa cum laude* in electronic engineering from the Second University of Naples, Italy, in 1998 and the Ph.D. degree in information engineering from the University of Naples Federico II, in 2002. Since December 2002, he has been with the Department of Biomedical, Electronic and Telecommunication Engineering, which, since January 2013, has been consolidated into the Department of Electrical Engineering and Information Technology, University of Naples Federico II. He first served as an Assistant Professor of signal theory and mobile communications and, since December 2011, has served as an Associate Professor of telecommunications. He has also held teaching positions at the Second University of Naples. His research activities lie in the broad area of statistical signal processing, digital communications, and communication systems. In particular, his current interests include cyclostationarity-based techniques for blind identification, equalization and interference suppression for narrowband modulation systems, code-division multiple-access systems, multicarrier modulation systems, space-time processing for cooperative and cognitive communications systems, and software-defined networks. Prof. Verde has served as an Associate Editor for the IEEE Transactions on Signal Processing since September 2010.